UNIVERSITÀ DEGLI STUDI DI PADOVA

Dipartimento di Psicologia Generale

Corso di laurea in Neuroscienze e riabilitazione neuropsicologica

Tesi di laurea magistrale

Elaborazione della magnitudine nell'illusione di Delboeuf classica e numerica

Unraveling magnitude processing in the classical and numerical Delboeuf illusion with electric insights

Relatore
Prof. Battaglini Luca

Correlatore
Prof. Granziol Umberto

Laureando:
Francesco
Carabba
Matricola:
20803030

Anno Accademico 2023/2024

Index

Abstract

Grasping the cognitive processes and neural mechanisms behind perceiving and processing quantities is crucial for uncovering the complexities of human cognition. The idea of a single magnitude system that includes non-symbolic number estimation as well as other magnitudes like time and space remains contentious, as there is still a lack of definitive evidence. Recent research has explored whether biases that impact spatial decisions also affect numerosity judgments, using visual illusions such as the Delboeuf illusion. The rationale being that if a shared cognitive system encodes both spatial and numerical processing, then these perceptual biases should similarly influence judgments related to numerosity and continuous quantities. While recent findings do support the idea of a generalized magnitude system, studies that directly compare the perception of the classic Delboeuf illusion with its numerical equivalent are still lacking. In this study, we aim to explore the possible existence of a generalized magnitude system by examining whether the same perceptual bias similarly influences the processing of different magnitudes. Additionally, participants received three sessions of transcranial alternating current stimulation (tACS) at different frequencies (7 Hz, 18 Hz, and placebo) to observe whether it affects the strength of the Delboeuf illusion similarly in its classical and numerical version. Based on previous findings, we specifically hypothesize that theta-frequency tACS will enhance visual integration, thereby intensifying the illusion, while beta-frequency tACS will decrease the strength of the illusion by promoting visual segregation. The results showed different performances in discriminating different quantities, with significantly higher discrimination ability observed when discriminating between areas. However, a significant correlation emerged between the two discriminations such as between the numerical and the classical Delboeuf illusion. Additionally, no significant interaction was observed between tACS stimulation frequency and discrimination, supporting the idea of a single mechanism underlying the processing of different magnitudes. Notably, contrary to our initial hypothesis, tACS at 7 Hz seems to reduce the strength of the perceptual illusion. These findings enhance our understanding of the cognitive processes involved in quantity perception and underscore the potential of noninvasive brain stimulation techniques for modulating visual perception.

Introduction

The approximate number system

The approximate number system (ANS) is an intuitive, abstract, and flexible system responsible for our sense of number. Historically it has been considered a specialized, domain-specific system for representing number which is phylogenetically ancient and used actively throughout life (Odic & Starr, 2018). The ANS underpins our ability to automatically and efficiently extract the approximate number of items in a scene regardless of sensory modality in which they are presented (Dehaene, 2009; Feigenson et al., 2004). In other words, the ANS generates nonverbal representations of numerosity (Halberda et al., 2012).

When the ANS is used, it manifests itself through two behavioral signatures (Figure 1). The first being scalar variability. This generally means that the more the numerosity presented increases, the more the estimate becomes variable. And more precisely means that variability in estimating numerosity increases linearly with number. For example, the variability in estimating 20 items is about twice as large as the variability in estimating 10 (Cordes et al., 2001). Variability signatures distinguish verbal from nonverbal counting for both large and small numbers. The second behavioral signature is ratio-dependent performance when deciding which of two sets is larger numerically (numerosity discrimination task), accordingly to Weber's Law. This means that if the ratio between the numerical magnitude of the two numerosity (max/min) increases the performance improves while if the ratio approaches 1 the performance worsens. For example, distinguishing 30 dots from 20 dots is significantly harder than distinguishing 30 dots from 10 dots. To measure ANS acuity, the Weber fraction (w) is often employed. Which is the smallest, and therefore most difficult, ratio that can be discriminated reliably (i.e. with a certain probability decided a priori).

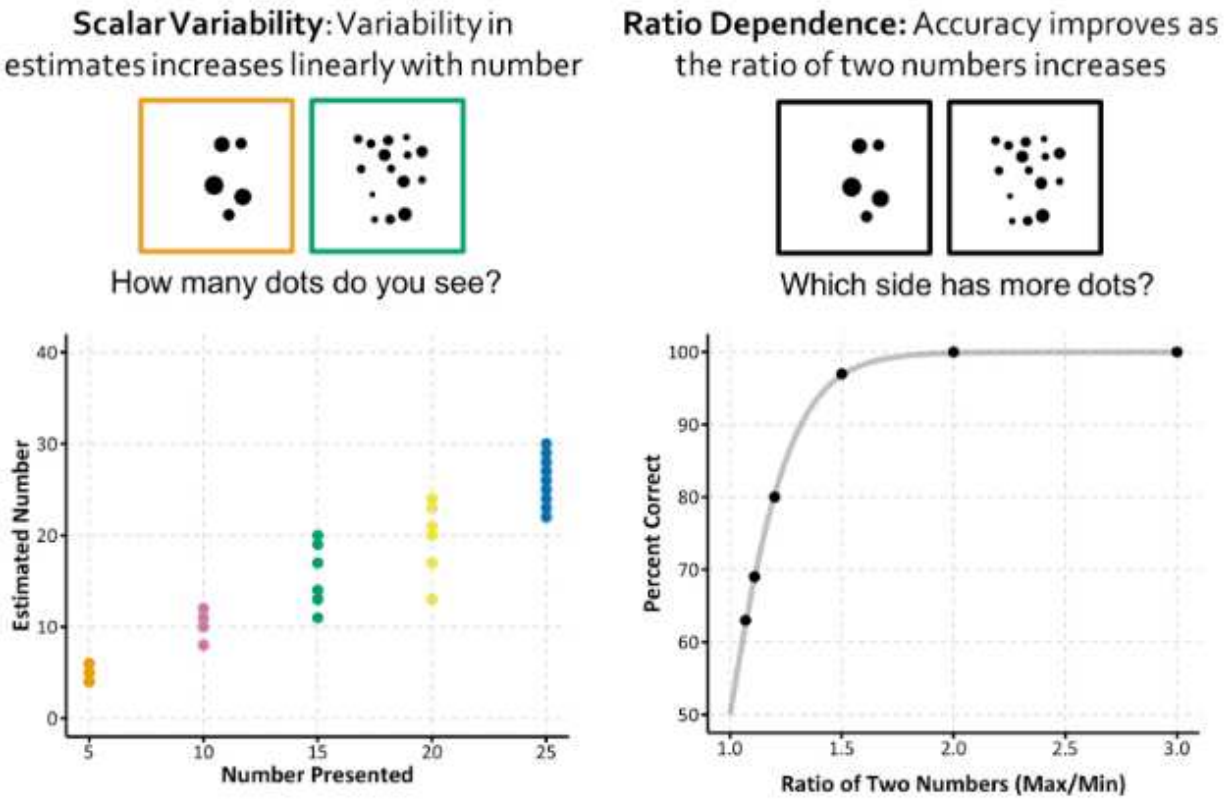

Figure 1. The two signatures of the approximate number system. On the left: scalar variability, where the variability increases linearly as the number of presented items increases. On the right: ratio dependency, where accuracy improves and reaction time decreases as the ratio between two numbers becomes larger (Odic & Starr, 2018).

These signatures suggest that the ANS represents numbers as noisy Gaussian curves along an ordered mental number line. Indeed, these key features of approximate number representations are embodied in models that depict numerosity as a fluctuating mental magnitude, comparable to a “number line”. There are two competing mathematical models of the number line (Figure 2), despite their behavioral predictions being very similar (Dehaene & Changeux, 1993; Feigenson et al., 2004; Gallistel & Gelman, 2000). The linear model with scalar variability depicts non-verbal number representations (the number line) as a series of equally spaced distributions that become more spread out as they increase. In other words, scalar variability implies that the signals encoding these magnitudes are 'noisy', fluctuating from trial to trial, with the signal distribution's width expanding in proportion to its mean. In essence the larger the magnitude, the noisier its representation becomes. On the other hand, the logarithmic model with fixed variability places successive numerosities on a

logarithmic scale, each subject to a consistent amount of noise. In both models, larger numerosities are represented by distributions that increasingly overlap with nearby values. This overlap raises the chances of confusing a target with its neighbors, resulting in ratio-dependent performance. Recent evidence suggests that the representation of numerical magnitude is initially logarithmic but becomes linear during the elementary school years (Siegler & Opfer, 2003).

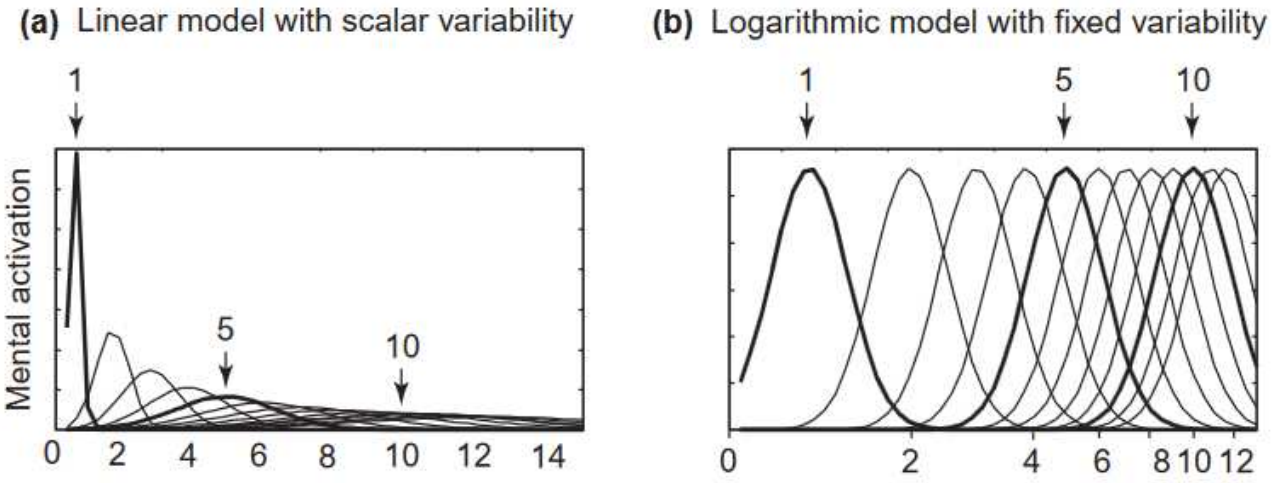

Figure 2. Two models of the mental number line, a linear model (a) and a logarithmic one (b), illustrating how mental activation varies with numerosity (Feigenson et al., 2004).

These signatures are useful because they allow us to identify different representations of numbers by observing whether scalar variability and ratio dependence are present. Let's look at an example. Evidence suggests the existence of two core systems for representing numbers. One system (the one we have already talked about and will refer to more often) represents large, approximate numerical magnitudes, while the other precisely represents small numbers of individual objects. Subitizing is thought to rely on this exact small-number representation system for tracking small quantities. The performance patterns between these two systems differ significantly: the large-number system exhibits ratio-dependent performance, whereas the small-number system depends on the absolute number of items presented, with an upper limit of 3 (Feigenson et al., 2002).

Individual and developmental differences in ANS performance are typically assessed by briefly displaying sets of dots or playing a quick series of tones, making counting impossible. Participants are then asked to compare this stimulus to another set of dots presented at the

same time. Infants are usually tested by habituating them to a certain number of dots or by observing their preference for looking at one of two streams of dots, with one stream remaining constant and the other varying in number. Each person's ANS acuity can then be determined by identifying the most difficult ratio they can accurately distinguish (usually the ratio for which the subject has a 75% probability of successful discrimination) (Odic & Starr, 2018).

The existence of ANS is observed across cultures, ages, and species of animals. For example, it is observed that newborns spontaneously associate stationary, visual-spatial arrays of objects with auditory sequences of events based on number. This provides evidence for abstract numerical representations at the start of postnatal experience (Izard et al., 2009). It is also observed that in cultures where there is no symbolic representation of numbers (number words), performance in a discrimination task depends on the ratio of the numerosities to be discriminated (Frank et al., 2008). Finally, there is evidence that when discriminating between two numerosity monkey's numerical capacity were systematically controlled by the ratio of the values compared (Cantlon & Brannon, 2006).

Consistent results from various approaches, species, and age groups indicate that the posterior parietal cortex, especially the intraparietal sulcus (IPS), plays a crucial role in processing numerical magnitudes. An electrophysiological study from Nieder & Miller (2004) used single-cell recording to show that in monkeys, during a visual numerosity judgment task, the highest proportion of neurons selective for numerosity was found in the IPS, with only a few such neurons present in other areas of the posterior parietal cortex (PPC) or the inferior anterior temporal cortex. Additionally, neurons in the fundus of the intraparietal sulcus responded to and conveyed numerosity information earlier than those in the prefrontal cortex (PFC), indicating that numerosity information likely flows from the PPC to the lateral PFC, suggesting a parieto-frontal network for processing numerosity in monkeys. Additionally, neural activity in these regions displays the same ratio-dependent characteristics of ANS representations observed in behavior (Piazza & Eger, 2016). Sensitivity to numerosity in the posterior parietal cortex develops early in human life, even before children learn to count or begin formal schooling. For instance, functional near-infrared spectroscopy has shown that activity in the right parietal cortex of 6-month-old infants is influenced by changes in the number of objects in an array but not by changes in shape (Hyde et al., 2010). Similarly, functional magnetic resonance imaging reveals that the IPS of 4-year-olds responds to numerical changes but not to changes in shape (Cantlon et

al., 2006). In adults, regions of the parietal cortex respond to numerical information regardless of whether it is presented as arrays of dots, Arabic digits, or auditory number words (Piazza et al., 2006). Children as young as six also show abstract numerical representations in the IPS (Cantlon et al., 2009). Overall, neuroimaging evidence indicates that the IPS supports amodal, abstract numerical representations, which appear early in development, demonstrating that the ANS develops before exposure to number words or formal math education.

A topic of great interest is the connection between the ANS and formal, symbolic math abilities, which are developed through explicit teaching and learned by only some individuals. A landmark study (Halberda et al., 2008) examined whether there are significant individual differences in ANS acuity and if these differences correlate to individual differences in symbolic math achievement. They found that subjects' ANS acuity, measured by Weber fraction (w), consistently correlated with their symbolic math performance from kindergarten through sixth grade on standardized math tests, even after controlling for various cognitive and performance factors (intelligence, working memory, and vocabulary size). These results showed that individual differences in formal mathematics ability are related to individual differences in the acuity in the number sense. However, since this is a retrospective study (it correlates ANS acuity of 14-year-old children with their past scores on standardized maths achievement tests) it is difficult to understand the direction of the relation between ANS acuity and symbolic math achievement. It could be that ANS, given its presence as early as infancy, plays a causal role in determining individual maths achievement. But it could also be that individual differences in the quantity or quality of engagement in formal mathematics might increase ANS acuity. Later a longitudinal study (Starr et al., 2013) explored this question in more detail. This study provides evidence that preverbal number sense in infancy can predict mathematical abilities in preschool-aged children. Specifically, numerical preference scores (a measure of ANS acuity in infants) at 6 months old were found to correlate with both standardized math test scores and nonsymbolic number comparison scores at 3.5 years old. This suggests that preverbal number sense aids in acquiring numerical symbols and mathematical skills. This correlation persisted even after accounting for general intelligence, highlighting that preverbal number sense uniquely contributes to mathematical ability. These findings support the hypothesis that an intuitive sense of number (preverbal, nonsymbolic numerical capacities), which exists before language, forms the foundation for learning to count and developing symbolic mathematical knowledge. A fascinating study (Halberda et al., 2012) investigated the

precision of basic numerical intuitions and their relation with school mathematics performance across the lifespan with a massive Internet-based sample of more than 10,000 participants aged 11 to 85. The study focused on how the precision of ANS representation and its relationship with formal mathematical abilities transforms during the lifespan. They found that ANS precision improves from ages 11 to 30, reaching a peak, followed by a steady decline from 30 to 85 years of age. Additionally, they observed a consistent, modest relationship between ANS precision and school mathematics ability throughout the lifespan. All this evidence suggests that ANS is a foundation on which symbolic number representations are constructed. For instance, children with more accurate ANS representations may find it easier to learn numerical symbols and their meanings, which can, in turn, support their early arithmetic learning (Van Marle et al., 2014).

The generalized magnitude system

Behavioral, neuropsychological, physiological, and neuroimaging studies have provided empirical evidence indicating an interaction between the representation of numerosity and the representation of continuous quantity like time and space. This has led to the hypothesis that the approximate number system (ANS) might also process continuous quantities, not just discrete numbers. In other words, it suggests the existence of a shared cognitive mechanism that encodes non-symbolic number estimation along with other magnitudes like time and space. While our study primarily concentrates on non-symbolic numbers (numerosity), it is important to remember that the representation of symbolic numbers is thought to arise from this fundamental number sense (Nieder & Dehaene, 2009). Therefore, the literature we review includes tasks involving both symbolic and non-symbolic numbers.

Behavioral evidence from the distance effect has highlighted a connection between space and numbers (Roitman & Brannon, 2003). This effect can be described as the phenomenon in which comparing two numbers becomes easier as the numerical gap between them increases. The distance effect persists even when the numerical gap remains constant but the numbers themselves vary in size. Additionally, it is observed with dots, words, or a combination of words and digits, not just numbers alone. Notably, this effect is also observed in nonhuman species (Dehaene et al., 1998; Roitman & Brannon, 2003). Furthermore, numerous behavioral protocols have demonstrated a strong link between numbers and space, where smaller numbers are positioned on the left side of space and larger numbers on the right. A demonstration of the connection between numbers and space is given to us by the spatial-numerical association of response code (SNARC) effect. In a parity judgement task, where participants classify numbers as even or odd, responses are faster for larger numbers when made on the right side and faster for smaller numbers when made on the left side. This number-space association happens even though the task does not involve numerical magnitude (Dehaene et al., 1993). A demonstration that merely presenting a digit automatically directs attention to either the left or right visual field (LVF/RVF) depending on the number's size is provided to us by (Fischer et al., 2003). In their study they showed single-digit numbers (1, 2, 8, or 9) at a central fixation point, followed by a target appearing in either the LVF or RVF, and participants were asked to respond as quickly as possible (detection reaction time). The number's presentation influenced the direction of attention

allocation, affecting detection reaction time. Digits 1 and 2 automatically directed attention to the LVF, facilitating responses to stimuli there, whereas digits 8 and 9 directed attention to the RVF, even though the digits were non-informative and irrelevant to the detection task. A third demonstration of automatic numerical-spatial interactions involves the bias in line bisection when the lines are made up of numbers (Calabria & Rossetti, 2005). When participants are asked to indicate the midpoint of a line composed of 'x's, they are generally accurate. However, when the line is composed of the digit 9 or the French word 'neuf' (nine), participants tend to deviate to the right. Conversely, when the line is composed of the digit 2 or the word 'deux' (two), participants deviate to the left. This suggests that numbers automatically influence attention towards the left or right, causing the bisection of the lines to deviate accordingly. The connection between time and numbers is supported by dual-task experiments, many of which report that a secondary task impairs time estimation (Casini & Macar, 1997). Indeed, time tasks are easily disrupted but, importantly, are not themselves good disrupters. However, one exception indicates that time and number share cognitive resources (Brown, 1997). Subjects were tested under three dual-task conditions: time and rotor tracking, time and visual detection, and time and mental arithmetic. All secondary tasks disrupted time estimation, but only mental arithmetic was impaired by the temporal task. This suggests that time and number may rely on common magnitude mechanisms, whereas the other two tasks primarily involve visual processing. Evidence of the connection between time and space is provided by the study conducted by De Long (1981) where subjects were asked to perform tasks in environments scaled to 1/6, 1/12, or 1/24 of actual size and to stop when they believed thirty minutes had passed. The results showed that the ratio of actual time passed to the estimated time varied in proportion to the scale of the environment.

Brain imaging studies have shown that spatial, numerical, and temporal processing involve activation of the parietal cortex (Dehaene et al., 1999; Rao et al., 2001; Simon et al., 2002). Specifically, spatial and temporal stimuli consistently activate the right inferior parietal cortex (IPC), while tasks involving numbers activate the parietal lobes bilaterally. Additional evidence for numerical-spatial interactions comes from the concurrent deficits in spatial and numerical processing often seen in patients with parietal lobe lesions. Classic studies on Gerstmann’s syndrome provide such evidence, showing that patients frequently experience both dyscalculia and spatial difficulties, including left-right confusion and finger agnosia. This syndrome is typically linked to lesions in the left angular gyrus (Gerstmann, 1940). Recent

research examining distortions in number processing in patients with hemi-spatial neglect due to right hemisphere brain damage further supports the intrinsic link between number and space. In a study, patients with neglect were asked to identify the midpoint number of various numerical intervals (such as the midpoint between 3 and 12). Remarkably, their responses skewed towards larger values, deviating to the right, even though both the problem and the responses were presented in a non-spatial, spoken format (Zorzi et al., 2002). Furthermore, neuropsychological studies have demonstrated that lesions in the parietal cortex not only lead to deficit in numerical and spatial processing but also lead frequently to concurrent temporal deficits (Critchley, 1953). Besides the overlapping brain regions linked to time, space, and number identified in neuropsychological and brain imaging studies, multiple studies utilizing transcranial magnetic stimulation (TMS) have revealed that stimulating the parietal cortex in human subjects can lead to deficits in spatial tasks (Bjoertomt, 2002), as well as in number comparison (Göbel et al., 2001) and time discrimination (Walsh & Pasual-Leone, 2003). In summary, evidence from deficits following TMS or brain lesions, along with activity observed in fMRI, PET and EEG studies, consistently indicates that common mechanisms for estimating space, time, and quantity are located in the right inferior parietal cortex.

Additional evidence is provided by neurophysiological studies such as that of Sawamura et al. (2002). The authors recorded the activity from the upper bank of the IPS and the superior parietal lobule in macaques and identified neurons that are selective for numerical quantity. These neurons are located in areas that are also spatially selective (Wilson et al., 1993). Additionally, studies on non-human primates have investigated the cortical processing of duration and observed activation in the inferior parietal lobe (Onoe et al., 2001). Thus, studies on non-human primates demonstrate that areas in the parietal lobule involved in spatial processing also contain neurons that are selective for numerical quantity and temporal duration.

This empirical evidence led (Gallistel & Gelman, 2000) to hypothesize that numerosity, amount, and duration should be represented using the same type of symbols (mental magnitudes), due to the frequent necessity of combining different kinds of quantity for important behavioral decisions. This hypothesis later inspired (Walsh, 2003) to develop “A Theory Of Magnitude (ATOM)”, proposing that time, space, and quantity are components of a generalized magnitude system, with the parietal cortex playing a crucial role. The core

idea of this theory is that the linking function of the many capabilities of the parietal cortex is the need to encode information about magnitudes of the external world that are used in action. Afterwards, numerous empirical evidence has shown how numerosity judgment can be affected by variations in unrelated continuous quantities and vice versa, consolidating this theory.

A study by Kaufmann et al. (2005) investigated the neural correlates of a number-size congruity task using an event-related fMRI design. They presented one digit number pairs in a number-size interference task that required subjects to focus on one stimulus property (e.g., numerical size) and to ignore the other (physical size). In different blocks, participants were asked to decide which digit of a digit pair was numerically larger (numerical comparison task) or physically larger (physical comparison task). Stimuli were divided into three categories: (a) congruent, where physical and numerical comparisons produce the same response; (b) incongruent, where physical and numerical comparisons produce different responses; and (c) neutral, where the stimuli vary only in the aspect relevant to the task. The behavioral results showed clear distance effects, with faster reaction times for greater distances compared to shorter ones, and size congruity effects, with slower reaction times for incongruent stimuli compared to congruent ones, across both tasks. Imaging results demonstrated that incongruent trials, as opposed to congruent trials, resulted in increased activation in the dorsolateral prefrontal cortex and the anterior cingulate cortex, which are areas linked to attentional control. The distance effect, in the neutral condition, led to greater activation in bilateral parietal regions, including the intraparietal sulcus (IPS). The primary aim of the authors was to identify the neural correlates of the number-size congruity task and to investigate if some of the activation observed was specific for processing numerical information. A similar bilateral activation of parietal and occipital areas was observed for both task, confirming the crucial role of the IPS in magnitude processing and supporting the notion that a common parietal region is responsible for encoding both number and size.

De Hevia et al. (2008) investigated whether numerical processing influences the mental representation of horizontal spatial extension using a length reproduction task. To test the hypothesis that numbers cause an illusory mis-estimation of spatial extent based on their magnitude, participants were shown a space delimited by two numbers and asked to reproduce that space as accurately as possible. The hypothesis predicted correctly that a space delimited by two small numbers (e.g., 1 1 and 2 2) would be reproduced shorter in length compared to the same space bordered by two large numbers (e.g., 8 8 and 9 9).

Length misestimations caused by Arabic numbers were viewed as a cognitive illusion, wherein the processing of magnitude information results in the expansion or compression of the mental representation of spatial extension.

In the same year Droit-Volet et al. (2008) compared how children aged 5 and 8 years, as well as adults, discriminate duration alongside other quantities, such as numerosity (discontinuous) and line-length (continuous). Using a bisection task, they examined discrimination with quantities presented both simultaneously (non-sequentially) and sequentially. The results indicated similar sensitivity to different quantities, suggesting that all quantities are represented by analogue magnitudes with scalar variability. Furthermore, these findings support the idea that the fundamental abilities to process various quantities emerge early, though discrimination of analogue magnitudes improves with age. Consistent with ATOM (Walsh, 2003), they propose that time, space, and number are all elements of a generalized magnitude system functioning from birth.

Further evidence for the connection between discrete and continuous quantity processing is provided by Gebuis & Reynvoet (2012). This study demonstrated that participants use various visual cues to estimate numerosity. Indeed, even after controlling for these cues (i.e. individual visual properties alone were not informative about numerosity) participants' estimations were influenced by the visual characteristics of the dot arrays. Specifically, they provided larger estimates when the dot arrays had smaller average dot diameter, aggregate surface area, or density, but a larger convex hull. This reliance on visual cues for numerosity estimation suggests that the existence of an approximate number system that operates independently of visual cues is unlikely. Instead, authors propose that humans estimate numerosity by integrating different visual cues present in the stimuli.

A study by Hayashi et al. (2013) investigated the neural substrates that mediate the interaction between numerosity and time. First, they performed an fMRI experiment and show that the right inferior frontal gyrus (IFG), right IPC, and bilateral occipital regions exhibit joint activation for numerical and duration processing in comparison tasks. The right IFG activity was modulated by congruency between these two dimensions of magnitude. Then, they conducted three TMS experiments to investigate the causality and specific roles of these regions in the numerosity-time interaction using duration discrimination and reproduction tasks. The results showed that disruption of the right IFG impaired duration discrimination, whereas disruption of the right IPC modulated the degree of the influence of

numerosity on time perception and also impaired time estimation accuracy. Together, these results suggest that, although the right IFG plays a role in the interaction at a decision stage, mixing of magnitude information at the perceptual level takes place in the right IPC. In summary, this study showed common neural representations of numerosity and time in two different brain regions.

Skagerlund et al. (2016) found similar results, they aimed to examine how the brain processes magnitude information across the dimensions of time, space, and number using an fMRI paradigm. The goal of this study was to explore the proposed existence of a generalized magnitude system by identifying any overlapping neural substrates among the investigated dimensions. Specifically, they hypothesized that the IPS and IFG regions would be crucial in the magnitude processing network, expecting these areas to show common activation across different tasks. They employed an fMRI paradigm with three experimental tasks focused on processing space, time, and numerosity. Initially, they assessed task-specific activation by comparing each task to its respective control condition. Following this, a conjunction analysis was conducted, revealing a set of cortical areas involved in all tasks. As predicted, the results showed that the right IPS was engaged in all three tasks, supporting the idea that the IPS may play a fundamental role in the magnitude processing system and serve as a central hub for the abstract representation of magnitude beyond just numerosity. Additionally, as predicted, the conjunction analysis revealed that the IFG was activated across all tasks. In conclusion, they identified several overlapping neural substrates across various magnitude dimensions and argue that these cortical nodes form a distributed magnitude processing system consistent with the ATOM account (Walsh, 2003).

All this evidence suggests the existence of a single and general cognitive system involved in the processing of different types of quantity, however, not everyone found similar results. Dormal et al. (2008) discovered a dissociation between numerosity and duration processing in the left IPS using off-line repetitive transcranial magnetic stimulation (rTMS). In the study, participants compared the numerosity of flashed dot sequences or the duration of single dot displays before and after 15 minutes of 1Hz rTMS over one of three sites: the left or right IPS or the vertex, which was used as a control site. Compared to the control site, performance was only slowed in the numerosity comparison task following left IPS stimulation, while duration comparison task performance remained unaffected for any parietal site. These results suggest, in disagreement with previously discussed evidence, that the parietal region critical for numerosity processing is not involved in duration

processing, revealing at least one brain area where duration and numerosity comparison processes are distinct. Furthermore Anobile et al. (2018) investigated the interactions between numerosity and size perception sensitivity. They measured two sensory parameters in children: perceptual adaptation and discrimination thresholds for both size and numerosity. The findings revealed no correlation across participants for either discrimination thresholds or adaptation strength for numerosity and size. This lack of correlation indicates separate mechanisms for numerosity and size perception, challenging the "sense of magnitude" theory and supporting the existence of a specialized "number sense".

Visual illusion: an instrument to study quantity processing

To shed light on the existence of a generalized magnitude system recent studies have used visual illusions to determine if perceptual biases that affect spatial decisions also impact judgments of numerosity. The rationale being that if the same cognitive system encodes both spatial and numerical abilities, these perceptual biases should similarly influence judgments about numerosity and continuous quantities.

Earlier research indicated that numerosity discrimination is affected by spatial cues like length, density, and surface area (De Hevia et al., 2008), implying a significant interaction between numerosity estimation and spatial perception. Building on this foundation, Dormal et al. (2018) aimed to investigate how perceived length influences numerosity estimation by employing the Müller-Lyer illusion. To explore how spatial cues are integrated into numerosity estimation, this study examined the interaction between length and numerosity under varying perceptual conditions (manipulating objective versus subjective length) and response modes (comparison versus estimation). The researchers hypothesized that the interference of length with numerosity is influenced by how the cues are perceived rather than by their objective properties. To test this, they employed a paradigm using the Müller-Lyer illusion, which manipulates the perceived length of dot arrays without altering their actual length. The Müller-Lyer illusion is a geometric illusion in which a straight line with outward-pointing arrowheads at its ends appears longer than an identical line with inward-pointing arrowheads (Müller-Lyer, 1889). Although subjective experience plays a role in perceptual decisions, research prior to this study has only altered the objective value of sensory cues to study numerosity extraction, neglecting the role of subjective experience in understanding the interaction between physical size and numerosity. Perceptual illusions offer a distinct experimental approach to tackle this issue, as they alter the subjective perception of specific physical variables while keeping the objective numerosity constant across different illusion conditions. In the comparison task, numerical biases emerged when the arrays appeared to differ in length due to the illusion. Additionally, during the estimation task, participants overestimated the number of dots when the array seemed longer because of the outward-pointing arrows. These results indicate that the illusory perception of length impacts numerosity estimation beyond the actual length. In other words, they reveal that the interaction between length and numerosity is driven by subjective perceptions of length rather than its objective measurement.

A study by Picon et al. (2019) aimed to investigate whether, and which, non-numeric features influence number perception. To minimize the potential for response conflicts, the researchers employed a number estimation task in addition to a discrimination task. If congruency effects (where participants seem biased by non-numeric features rather than the number itself) are absent in number estimation tasks, it would suggest that the congruency effects seen in standard discrimination tasks are likely due to a Stroop-like response conflict. Conversely, if congruency effects persist even with the estimation task, it would indicate that non-numeric features are indeed involved in number perception itself, independent of any response conflicts. To specifically target certain non-numeric features, the authors incorporated stimuli into well-known visual illusions: the plug-hat illusion, which primarily affects the perception of contour length (Simanek, 1996), and the Ebbinghaus illusion, which selectively influences the perceived convex hull of objects. In the plug-hat illusion, participants perceive a circular contour or arc as significantly shorter than an identically long straight line. In the Ebbinghaus illusion, an object surrounded by smaller circles is perceived as significantly larger than the same object surrounded by larger circles. By using these visual illusions, the researchers were able to preserve the objective differences in the stimuli while allowing the participants' subjective perception of non-numeric dimensions to be influenced. This approach enables the precise targeting of specific non-numeric features without altering the other objective non-numeric features within the display. In a series of experiments, the researchers compared performance on number discrimination and number estimation tasks by embedding numerical displays within visual illusions and manipulating two specific non-numeric features: contour length and convex hull/density. In these experiments, participants viewed dot displays where the side with more dots also had an (illusory) longer contour length or a (illusory) larger convex hull (congruent trials), and displays where the side with fewer dots had the longer (illusory) contour length or larger (illusory) convex hull (incongruent trials). As in previous studies, they anticipated that participants would perform better on congruent trials in the discrimination tasks. The crucial test was whether these biases favoring the congruent trials would also persist in the estimation task, where binary responses are removed. To summarize, this series of experiments revealed two key findings: (1) Embedding dots within a contour length illusion (i.e. the plug-hat illusion) resulted in a significant congruency effect during the discrimination task, but no such effect was found in the estimation task. This suggests that contour length induces a Stroop-like response conflict with number, rather than directly influencing its encoding. (2) When dots were embedded in a display that varied in convex hull and/or

density (i.e. the Ebbinghaus illusion), a strong congruency effect was observed in both discrimination and estimation tasks, indicating that response biases alone do not fully explain why participants rely on convex hull during number perception. These results suggest that number is likely not a primary visual feature of perception, but instead is derived from a combination of other features, supporting the domain-general encoding theory. Indeed, the visual features used to encode convex hull and/or density seem to also be involved in encoding number, which challenges the domain-specific encoding theory.

Similar to the studies previously discussed, Pecunioso et al. (2020) sought to determine whether perceptual biases that influence spatial estimation also affect numerical estimation, which would support the idea of shared cognitive processes for space and number in the brain. Specifically, the authors aimed to explore whether non-symbolic numerical estimation varies depending on whether stimuli are presented vertically or horizontally. This hypothesis stems from the observation that many researchers have documented differences in perception between the horizontal and vertical axes in spatial tasks (anisotropy of perceived space) (Higashiyama, 1992). Given the pronounced asymmetry in how vertical and horizontal dimensions are perceived, it is reasonable to question whether a similar effect might be observed in non-symbolic numerical estimation. If spatial and numerical abilities indeed share a common cognitive framework, then perceptual biases influencing spatial judgments could also affect numerosity judgments. The horizontal–vertical (HV) illusion provides strong evidence for the anisotropy of perceived space. In its classic form, the illusion involves an inverted T figure where the horizontal and vertical lines are equal in length. Despite this, most observers perceive the vertical line as longer than the horizontal one (Avery & Day, 1969). This illusion appears to be linked to the shape of the human visual field, which resembles a horizontally oriented ellipse with a horizontal-to-vertical aspect ratio of 1.53. Interestingly, the HV illusion is also influenced by a factor unrelated to the anisotropy of perceived space: the ‘length bisection bias.’ This bias occurs when a line bisected by another line appears shorter than the unbisected line (Finger & Spelt, 1947; Mamassian & De Montalembert, 2010). To test the impact of the length bisection bias, researchers use an L-shaped version of the HV illusion, which involves both vertical and horizontal axes but avoids line bisection. Studies comparing performance on the T and L versions of the HV illusion have found that the T version leads to a greater misperception of length. To test their hypothesis, the authors utilized a visual pattern composed of white and black dots arranged in inverted T and L shapes to create an HV illusion. In control trials, black and white dots

were randomly distributed within the array. However, in test trials, white dots were aligned along one line (e.g., the vertical line), while black dots were aligned along the other (the horizontal line). Participants were asked to verbally estimate the number of white dots. The authors made two predictions: If numerical and spatial abilities share a common magnitude system, one would expect (1) an overestimation of white dots when they are presented on the vertical axis and (2) a stronger illusory effect in the inverted T pattern compared to the L pattern, due to the length bisection bias. Indeed, participants' accuracy differed depending on whether the target dots were presented entirely on the vertical axis, entirely on the horizontal axis, or randomly across both axes. Notably, the significant difference between the horizontal and vertical conditions suggests that items on the vertical axis were less underestimated than those on the horizontal axis. This finding is consistent with the anisotropy of vertical space observed in the HV illusion. The second prediction was also confirmed: when white dots were arranged in a vertical line, participants underestimated the number of dots less in the T shape than in the L shape. Therefore, the T shape appears to enhance the overestimation of vertically arranged dots. In conclusion, this study demonstrated a differential perception of numerosity in vertical versus horizontal spaces, reinforcing the notion that similar cognitive systems underlie both spatial and numerical estimation.

Following this evidence, Santacà & Granziol (2023) investigated whether non-symbolic numerical estimation varies according to perceived area size in both humans and non-human animals. To accomplish this, the researchers used the Delboeuf illusion to alter the perceived area size of square arrays without changing their actual size. The Delboeuf illusion is a well-known size illusion in which the perceived size of a target item is influenced by its surrounding context. In the classic version of this illusion, two identical target circles are surrounded by larger and smaller circumferences (Figure 3b). Humans tend to underestimate the size of the circle within the larger circumference and overestimate the size of the circle within the smaller one. The authors adopted a numerical version of the Delboeuf illusion (the same numerosity presented in two different contexts, Figure 3a) and anticipated that if numerical and spatial abilities share a common magnitude system, the arrays perceived as larger due to the Delboeuf illusion would also appear more numerous. The authors controlled for non-numerical continuous variables to prevent the use of non-numerical cues in discriminating numerosities and employed a relative two-choice discrimination procedure for both species. Specifically, humans were instructed, and fish

were trained, to select a target numerosity (either larger or smaller) during control trials where the arrays genuinely differed in their numerosity. Alongside these control trials, participants were also presented with illusory trials where the same numerosity was shown in two different contexts (a large and a small background) mimicking the Delboeuf illusion. When presented with two identical arrays, both humans and fish exhibited numerical biases, indicating that the illusion caused the numerosity of the squares in the two arrays to appear different. Since there were no differences in the illusory perception of the two quantities (area and numerosity), it can be speculated that their estimations are encoded by the same magnitude system. This finding aligns with the hypothesis of a common magnitude system underlying numerical and spatial abilities.

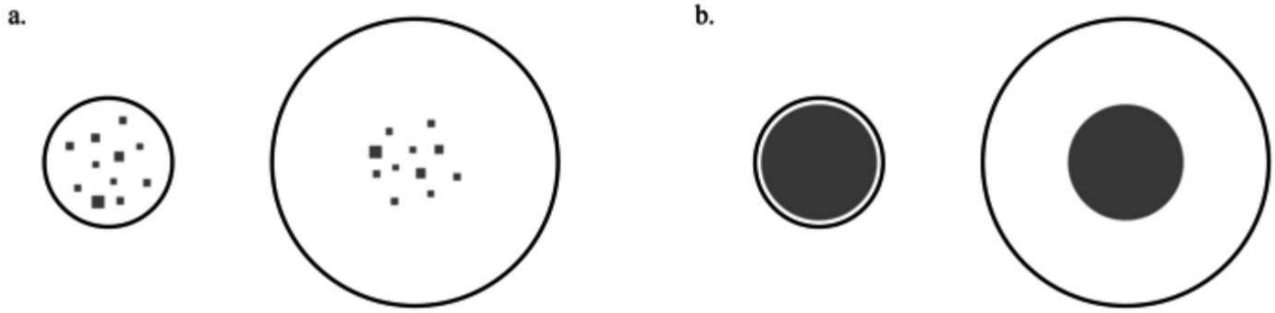

Figure 3. The figure shows both a numerical version (a) and a classical version (b) of the Delboeuf illusion, where either the same numerosity or the same target area is surrounded by two different contexts. Humans generally tend to underestimate the numerosity and target area within the larger ring, while overestimating those within the smaller ring.

In this study, participants were tested using the numerical version of the Delboeuf illusion (the same numerosity presented in two different contexts, Figure 3a) and not the classical version (the same area shown in two different contexts, Figure 3b). As a result, it was not possible to determine whether there was a correlation between the perception of the classical Delboeuf illusion and its numerical counterpart. This raises the question of whether the magnitude of the Delboeuf illusion is consistent across both types of quantities and, thus, if this perceptual bias similarly affects spatial decisions and judgments of numerosity. The aim of this study is precisely to answer this question.

Transcranial electrical stimulation and visual crowding

In this study our goal is to investigate the existence of a single cognitive system responsible for processing different quantities not just at the behavioral level, by examining whether the perceptual bias associated with the Delboeuf illusion similarly affects numerosity judgments and spatial decisions, but also at the neural level. To accomplish this, we intend to use transcranial alternating current stimulation (tACS) during behavioral tasks, aiming to modulate the strength of the Delboeuf illusion by applying different tACS frequencies. We will then compare whether this modulation occurs similarly and to the same degree for both types of illusions. Such findings would further reinforce the hypothesis of a generalized magnitude system. The reason we intend to use tACS in particular to modulate the strength of the Delboeuf illusion lies in its ability to influence the phenomenon of visual crowding, and will become clearer later. In fact, in the next sections we will delve into tES techniques (with special reference to tACS), the phenomenon of visual crowding, and the effect of tACS on this phenomenon in order to make clear the rationale behind the use of this technique and our hypotheses about its effect on the perception of the illusion.

Non-invasive brain stimulation (NIBS) techniques offer researchers and clinicians an effective tool to influence the activity of specific brain regions in humans, aiding in the investigation of the relationships between brain and behavior and promising to advance treatments for various neurological and psychiatric disorders (Yavari et al., 2018). Transcranial Electrical Stimulation (tES) and Transcranial Magnetic Stimulation (TMS) are two widely recognized types of NIBS, each affecting neural activity through distinct electromagnetic mechanisms. The acute effects of these two NIBS methods distinguishes them. TMS produces brief, high-intensity electromagnetic currents in the cerebral cortex, leading to supra-threshold neuron activation. In contrast, tES does not trigger action potentials in neurons but instead modulates their spontaneous firing activity by altering resting membrane potentials below the threshold (Nitsche & Paulus, 2000). TMS offers better spatial and temporal resolution, while tES is typically more affordable, simpler to use, and easily adaptable for double-blind, sham-controlled studies. Both methods serve as valuable complementary tools in neuroscience research, with the potential to address a key limitation of neuroimaging techniques: the challenge of determining the causal role of specific brain areas or functional networks in motor, perceptual, or cognitive processes

(Yavari et al., 2018). tES involves administering a low-intensity current (typically ~1-2 mA) through a battery-powered stimulator between two electrodes (anode and cathode) placed on the scalp (Figure 4). These electrodes are usually large, conductive rubber sheets encased in saline-soaked sponges. The current travels through the scalp and crosses the extracortical layers to reach the cortex, where it alters the membrane polarity of neurons in the underlying neural tissue. When direct current is applied, it flows from the anode to the cathode, leading to changes in the electrical activity of neurons and thereby modifying their synaptic efficiency. Although this modification does not generate action potentials, it is sufficient to alter the response threshold to a stimulus of the stimulated neurons (Brunoni et al., 2011).

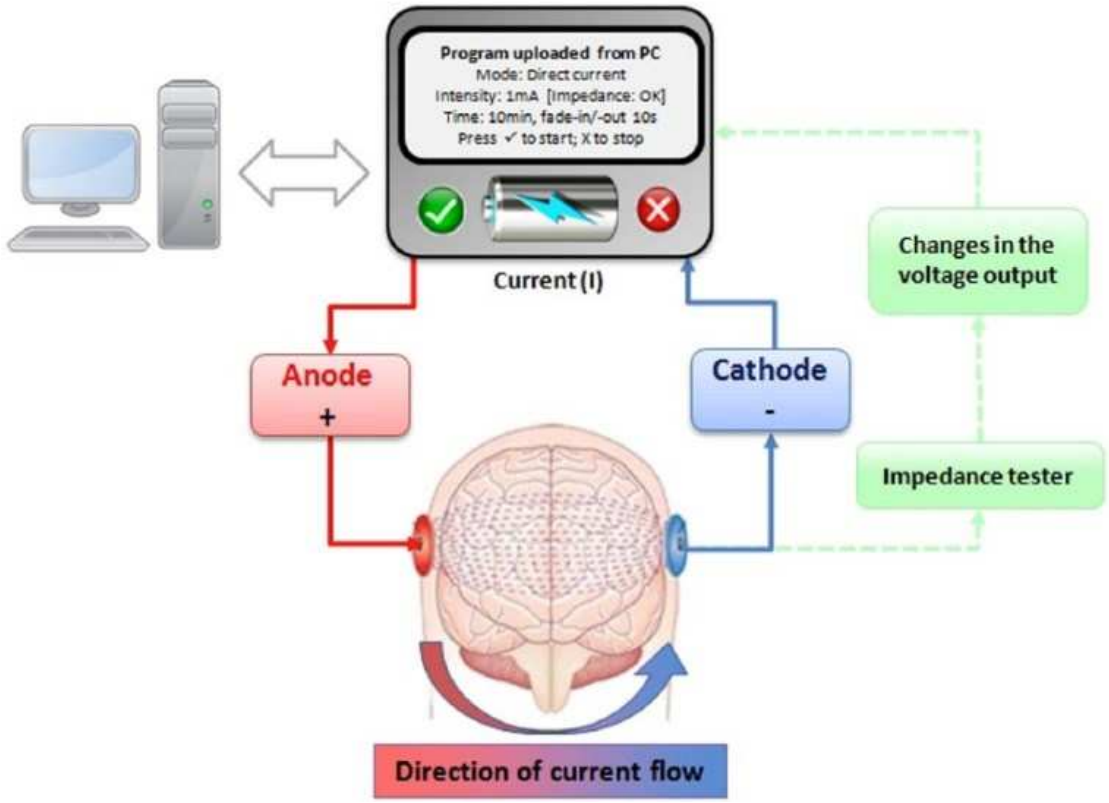

Figure 4. Schematization of the tES device (Yavari et al., 2018).

tES influences neuronal states using various transcranial current waveforms, with the most commonly used forms being direct (tDCS), alternating (tACS), and random noise (tRNS) stimulation (Figure 5). In anodal and cathodal transcranial direct current stimulation (tDCS), the current applied is direct and monopolar. Single-neuron recordings have shown that applying a direct current can depolarize (anodal stimulation) or hyperpolarize (cathodal stimulation) the neuronal membrane potential, thereby enhancing or reducing the neuronal

firing rate (Gartside, 1968). Therefore, we can be fairly confident that at the cellular level, direct current influences membrane excitability in opposite ways depending on the polarity of the stimulation. Moreover, these polarization effects continue after the tDCS session ends (Bindman et al., 1964), with the after-effects involving glutamatergic N-methyl-D-aspartate receptors (Liebetanz, 2002), which could indicate long-term potentiation-like mechanisms. Transcranial random noise stimulation (tRNS) involves the application of alternating currents across a range of frequencies, typically from 0 to 1000 Hz, although a narrower frequency band (e.g., 100 to 600 Hz) can also be used. It has been suggested that this repeated random subthreshold stimulation could increase sodium influx, leading to prolonged depolarization and the induction of long-term potentiation-like effects (Fertonani et al., 2011).

But let us delve deeper into tACS since, for reasons that will become clearer later, it is the technique adopted in this study. The synchronized and periodically shifting equilibrium between excitatory and inhibitory neural circuits gives rise to neural oscillations. These rhythmic patterns of brain activity are crucial for a wide range of physiological and behavioral processes in the sensory, motor, and cognitive domains (Fiene et al., 2020; Wischnewski et al., 2016). Additionally, irregular oscillatory patterns have been linked to various psychiatric and neurological disorders (Ahn et al., 2019; Benussi et al., 2022). Consequently, the development of tools like tACS, which can non-invasively generate oscillatory electric fields to influence neural spike timing and synaptic plasticity, holds significant promise for both research and therapeutic applications.

During tACS, weak oscillating electric currents are applied to the scalp. As these currents travel towards the brain, they are partially diverted by the surrounding tissues, such as the skin, skull, and cerebrospinal fluid (CSF). Although the resulting fluctuating electric fields are not strong enough to trigger action potentials in neurons at rest, they are comparable in magnitude to intrinsic local field potentials (LFPs), typically ranging from 1 to 4 mV/mm (Liu et al., 2018). Consequently, rather than inducing action potentials directly, tACS causes rhythmic changes in neuronal membrane potentials, influencing spike timing (Anastassiou et al., 2011). Evidence that weak extracellular oscillating electric fields can alter neuronal activity comes from studies conducted on anesthetized rodents and rodent brain slices (Alekseichuk et al., 2022; Vöröslakos et al., 2018), as well as research involving non-human primates (Krause et al., 2022) and human studies with surgical epilepsy patients, where invasive brain recordings are possible (Huang et al., 2017; Opitz et al., 2016). This is crucial since non-invasive recordings using magnetoencephalography (MEG) or

electroencephalography (EEG) are often significantly affected by technical artifacts from tACS (Kasten & Herrmann, 2019). These empirical findings demonstrate that oscillatory electric fields induce fluctuations in neuronal transmembrane potentials and significantly entrain neural activity.

Thus, tACS enables the entrainment of neural populations, where entrainment involves the temporal synchronization of ongoing brain rhythms with the externally applied alternating current (alignment of neural oscillatory rhythms with the frequency imposed by electrical stimulation). However, more recent studies emphasize the presence of additional complex and non-linear interactions between the applied sinusoidal current and the ongoing neural spiking activity (Krause et al., 2022). Although entrainment effects are generally dependent on frequency, the relationship between stimulation frequency and the neurophysiological response is complex and remains an area of ongoing research (Jefferys et al., 2003). One hypothesis proposes that stimulation frequencies that closely align with the brain's natural frequency are most effective, following the Arnold tongue phenomenology, which suggests that the closer the match between intrinsic and external oscillations, the less force is required to achieve entrainment (Huang et al., 2021). Therefore, the specific cytoarchitecture and the balance between excitatory and inhibitory activity within a region play a significant role in determining its susceptibility to tACS (Francis et al., 2003). There is also evidence suggesting that tACS can induce neuroplastic effects. For example, studies have shown that applying alpha tACS over the visual cortex increases alpha power visual evoked responses even after the stimulation has ended (Kasten et al., 2016). Moreover, one study provided direct evidence that tACS can mediate synaptic plasticity through N-methyl-D-aspartate (NMDA) receptors (Wischnewski et al., 2019). In this study, sensorimotor stimulation at 20 Hz increased motor-evoked potentials and EEG spectral activity in humans for up to 60 minutes after tACS, but these after-effects were suppressed when an NMDA receptor antagonist was administered. These findings support the hypothesis that tACS influences spike timing-dependent plasticity (Wischnewski & Schutter, 2017). Given its potential to modulate behavior, tACS holds significant promise as a cost-effective clinical tool for treating psychiatric and neurological disorders (San-Juan et al., 2022). In summary, tACS can selectively influence ongoing neural synchrony and induce neuroplasticity in specific brain areas or networks in a context specific way, meaning that can only modulate existing neural oscillations and cannot initiate new activity in brains that are in a steady state (Wischnewski et al., 2023).

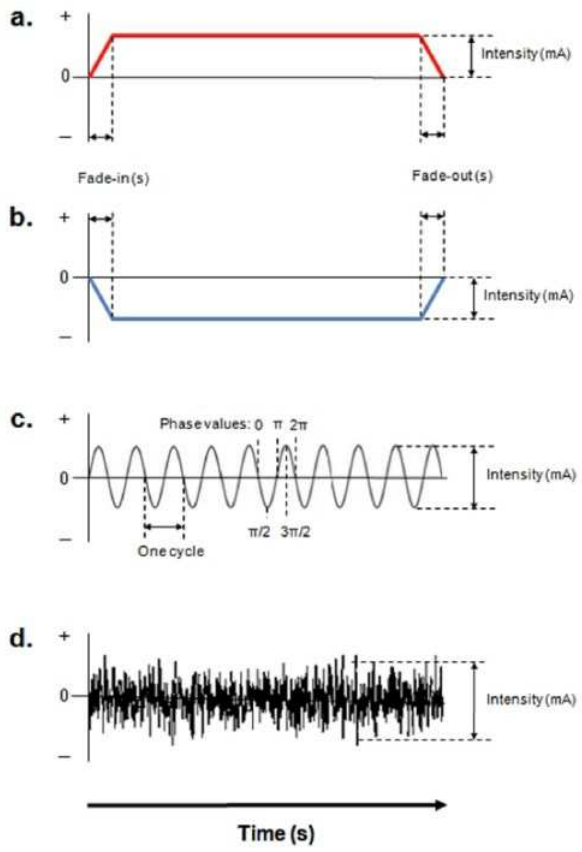

Figure 5. tES waveforms (Yavari et al., 2018).

In simple terms, the general idea is that while anodal tDCS and tRNS tend to increase neuronal excitability and potentially enhance behavioral performance, cathodal tDCS usually reduces neuronal excitability, leading to a decline in performance. Meanwhile, tACS can boost neuronal excitability by entraining the desired neuronal firing frequency, thus modulating performance (Paulus, 2011). However, this relationship is not always straightforward. Jacobson et al. (2012), through their meta-analysis, highlighted that tES does not operate in such a linear fashion and demonstrated that numerous factors, many of which are likely still unknown, can influence the outcomes, often leading to unexpected effects, particularly in the cognitive domain. According to the Network Activity-Dependent Model of tES effects, the impact of stimulation is influenced not only by the stimulation parameters (such as the type of current, intensity, duration, pauses, current direction, electrode type, and prior exposure to tES) but also significantly by the ongoing activity (i.e., the excitability state) of the targeted networks. Several studies have shown that tES can modulate behavior based on the neural activity level induced by the task, with the same type

of tES potentially having opposite effects depending on the degree of network engagement (Antal et al., 2004; Benwell et al., 2015; Bortoletto et al., 2015). Therefore, the level of network activity is a crucial factor in predicting the final outcome of tES. Stochastic resonance offers a useful framework for understanding the general online neuromodulation effects of tES. A key aspect of this mechanism is the assumption that tES does not apply a focal current; instead, it influences the activity of not only the neurons involved in executing a specific process or function but also the entire stimulated area. Under this assumption, the electric field introduced by tES can be considered as noise (due to its nonspecific nature) and a subthreshold signal within a network of neurons. Consequently, this noise will primarily affects neurons that are closer to their discharge threshold, meaning its effects are dependent on the network's activity level (Miniussi et al., 2013). This model predicts that adding noise to nonlinear systems can either enhance or impair signal detection, depending on the relationship between the state of the signal (i.e., the level of network activation) and the amount of noise introduced by tES (Kitajo et al., 2003; Miniussi et al., 2013). Therefore, according to this perspective, tES induces weak currents in the brain, injecting random activity (noise) into our self-organizing, nonlinear dynamic system. Depending on the intensity of the tES-induced activity (noise) and the state of the system, this may either facilitate or inhibit the emergence of a supra-threshold signal, leading to a subsequent improvement or decline in behavioral performance. The ongoing network state and its topology play a more significant role in determining the brain's response to stimulation than the stimulation parameters themselves. In the context of rehabilitation, this means that tES should not be viewed as a standalone treatment but rather as a support tool integrated into the broader rehabilitation protocol. Learning (synaptic potentiation) is not a passive outcomes of altering cortical activity through tES; it is driven by experience (Blais et al., 2008; Cho & Bear, 2009).

At present tES has some limitations and Bestmann & Walsh (2017) highlighted some of them. The first limitation relates to the assumed physiological effects of tDCS. The primary rationale behind using tDCS in cognitive studies is based on the idea that anodal or cathodal stimulation over the motor cortex (M1) leads to excitation or inhibition, respectively, and that these effects can be similarly observed in other cortical areas. However, there is limited evidence to support this assumption. Another significant issue concerns the cortical state in which these effects are observed. The excitability of the motor cortex is typically measured when the muscle is relaxed, but simply activating the muscle can alter the effects of

stimulation. Comparing this to the prefrontal cortex, it is challenging to equate a relaxed muscle with a relaxed cognitive state. Moreover, if muscle activation changes the effects of tDCS, it raises the question of how these effects will change in prefrontal areas during cognitive tasks, assuming the logic that what applies to M1 applies to the entire cortex. The second limitation involves the assumed effect of increasing stimulation intensity (dosage). The logic that sometimes is used is that the motor cortex serves as a model for the entire cortex, that anodal and cathodal stimulation is excitatory and inhibitory respectively, and that higher current leads to stronger polarity-specific effects. However, even if we accept the assumption that M1 represents the rest of the cortex, research on M1 indicates a non-linear or even non-monotonic dose-response relationship. Thus, there is little evidence that increasing the intensity of stimulation simply leads to an increase in the effect in a linear fashion. The third limitation pertains to the translation of the tES effect from the healthy population to the clinical populations. It is often overlooked that the physiological effects of tES observed in animals and healthy humans, which form the basis for its use in treating diseases, may not directly apply to patients. For instance, many psychiatric disorders involve alterations in neuromodulatory systems, and in patients with brain damage, factors such as the distribution of current flow and the condition of peri-lesional tissue can be significantly altered. How these factors influence the effects of tES remains unclear, but they are likely to be crucial. This raises the concerning possibility that the effects of tES observed in healthy brains may not translate straightforwardly to patient groups, as their brains may respond differently to stimulation.

We have already mentioned that one of the reasons we intend to use tACS to modulate the strength of the Delboeuf illusion is its ability to modulate the phenomenon of visual crowding. Let us therefore take a closer look at this phenomenon. Crowding is typically described as the negative effect of nearby contours on visual discrimination, representing a form of inhibitory interaction that is common in spatial vision. It hinders the ability to identify objects within clutter, not by lowering the apparent contrast, but by making the crowded targets indistinct or merged together (Levi, 2008). An example of this phenomenon is observed when a letter, presented in peripheral vision, that is easily recognizable on its own becomes unidentifiable when surrounded by other letters (Figure 6). This effect persists even with significant distances between the target and surrounding characters (Levi et al., 1994; Toet & Levi, 1992). In contrast, in foveal vision, crowding typically occurs only over very short distances (4-6 arc minutes, e.g.; Liu & Arditi, 2000; Toet & Levi, 1992) or may not occur at

all (Strasburger et al., 1991). Crowding effects have been observed across a wide range of tasks, including letter recognition (Toet & Levi, 1992), Vernier acuity (Levi et al., 1985), orientation discrimination (Westheimer et al., 1976), stereoacuity (Butler & Westheimer, 1978), and face recognition (Louie et al., 2007). Crowding also occurs with moving stimuli (Bex & Dakin, 2005). However, there are significant exceptions; for instance, crowding has little to no impact on the simple detection of a target (Livne & Sagi, 2007).

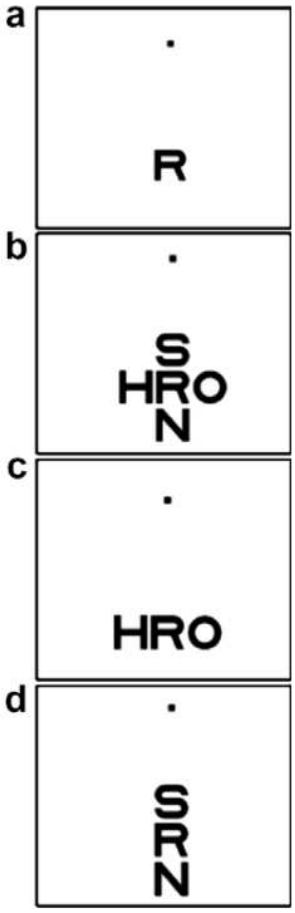

Figure 6. Crowding example with the letter “R” as the target and the other letters as the flankers. To experience crowding, fixate on the dot and try to identify the target letter under different conditions: when it appears alone (a), surrounded by four random flanking letters (b), surrounded by two random flanking letters placed horizontally (c), and surrounded by two random flanking letters placed vertically (d) (Levi, 2008).

Typically, crowding experiments aim to measure the "critical spacing," which is the distance at which surrounding elements impair performance, and to compare this under various conditions. Recent studies have manipulated both target size and eccentricity (the distance between the target and the fixation point) and found that the extent of peripheral crowding

(i.e., the critical spacing) remains largely constant regardless of target size (Levi, Hariharan, et al., 2002; Pelli et al., 2007). However, critical spacing is influenced by eccentricity, meaning it scales with the distance from the fixation point.

The strength and extent of peripheral crowding are significantly greater than those of masking (Levi, Hariharan, et al., 2002). Therefore, in peripheral vision, the suppressive spatial interactions caused by nearby flanks are unlikely to result from simple contrast masking. Nevertheless, although masking and crowding are distinct phenomena likely involving different neural processes, they both occur when a target is surrounded by other features, making the target harder to see, which can sometimes lead to confusion between the two. To differentiate them, Pelli et al. (2004) proposed a diagnostic test, based on the criterion that the critical spacing for crowding scales with eccentricity regardless of signal size, whereas for ordinary masking, it scales with signal size independently of eccentricity. In contrast, in the normal fovea, the extent of crowding is proportional to stimulus size and is not easily distinguishable from ordinary masking (Levi, Klein, et al., 2002). In summary, in peripheral vision, crowding is proportional to eccentricity, size-invariant, and distinctly different from ordinary masking. Another characteristic of this phenomenon is that crowding in peripheral vision is not isotropic. In the lower visual field, vertically arranged flanks (Figure 6d) cause more interference than horizontally arranged flanks (Figure 6b), whereas in the left visual field, the opposite pattern is observed (Levi, 2008). Toet & Levi (1992) demonstrated both the significant increase in the extent of crowding fields with increasing eccentricity and the variation in crowding fields depending on the orientation of the flanks. They found that, on average, crowding extends from about 0.1 times the target eccentricity in the tangential direction to 0.5 times the target eccentricity in the radial direction (Figure 7). Additionally, Bouma (1970) noted in his study that two flankers (one on each side of the target letter) were much more disruptive than a single flanker. Therefore, in peripheral vision, crowding is both inhomogeneous and asymmetric. Several studies have attempted to understand whether and to what extent the similarity between target and flankers influences the phenomenon of crowding. These studies have shown that crowding strongly depends on the similarity between the target and flankers, with crowding being more pronounced and widespread when the target and flankers are similar. Relevant dimensions of similarity include shape and size (Levi et al., 1994), orientation (Hariharan et al., 2005; Levi, Hariharan, et al., 2002), spatial frequency (Chung et al., 2001), depth (Levi et al., 1994), color (Bouma, 1969), and motion (Banton & Levi, 1993). Interestingly, empirical evidence

indicates that crowding is unaffected by whether the target and flanks are presented to the same eye or to different eyes (Flom et al., 1963; Levi et al., 1985, 1994). The occurrence of crowding even when the target and flanks are presented to separate eyes suggests that the interaction takes place at or beyond the point where information from both eyes is combined. To explain visual crowding, a two-stage model has been proposed (Levi, 2008). In the first stage, simple features are detected, possibly in the primary visual cortex (V1). The second stage involves integrating or interpreting these features as an object at a processing level beyond V1. During crowding, the target and flanker features are detected independently, but when both fall within the “integration field” (a second-stage receptive field), they merge into a percept that often appears jumbled or indistinct. According to this model, crowding results from limited processing resources.

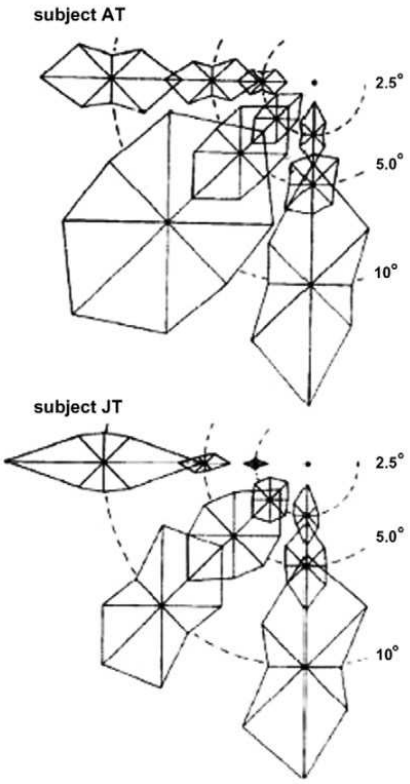

Figure 7. The two-dimensional shape of crowding in foveal vision, shown as the small dot at the center, and in peripheral vision at 2.5, 5, and 10 degrees (Toet & Levi, 1992).

An intriguing question is whether crowding affects everyday life. Since we navigate cluttered visual environments, crowding renders most objects in our peripheral vision unrecognizable. Understanding crowding can provide insights into modeling object recognition in both normal and impaired vision (Neri & Levi, 2006; Pelli et al., 2004). One key activity impacted by

crowding is reading. In individuals with normal vision, reading with peripheral vision is slow, and merely scaling the letter size and spacing does not counteract the reduction in reading speed with increasing eccentricity (Chung, 2002; Chung et al., 1998). Furthermore, recent studies (Levi et al., 2007; Pelli et al., 2007) indicate that the critical spacing for reading matches the critical spacing for crowding, again suggesting that crowding may be a limiting factor in reading ability. Another intriguing and practical question is whether practice can reduce the effects of crowding. The most compelling evidence for learning to reduce crowding comes from a study by Chung et al. (2007). In this study, eight observers were trained to identify crowded letters through repeated trials (6,000 trials) of recognizing the middle letters in trigrams. Notably, the critical spacing (the letter separation required for 50% correct identification of the target letters) significantly decreased (on average, by 38%) for both the trained and untrained separation distances.

In conclusion, crowding represents a significant bottleneck for object perception, particularly impairing object recognition in peripheral vision. It is a nearly universal phenomenon in spatial vision, and masking does not adequately explain it. There is an emerging consensus around a two-stage model, where the first stage involves the detection of simple features (possibly in V1), and a second stage is needed for the integration or interpretation of these features as an object beyond V1. Processes such as segmentation, selection, feature binding, and contour integration all seems to play a role in this. A comprehensive understanding of crowding could reveal the constraints on object recognition and clarify the principles that guide the integration of features into coherent objects.

Until now, we have explored several features of visual crowding without delving into the neural correlates of this phenomenon. While numerous psychophysical studies have explored the factors that influence crowding, and a two-stage model (previously discussed; Levi, 2008) has been proposed, the neural basis of this phenomenon remains unclear. Crowding might occur at an early stage of visual perception (such as the striate visual area, V1), where local features are integrated into more complex percepts (Pelli, 2008). Alternatively, higher visual areas (such as V4) could play a more significant role (Liu et al., 2009; Motter, 2006). Identifying the neural underpinnings of visual crowding would provide a clearer understanding of the mechanisms responsible for this effect. In the last period several studies have tried to shed light on this fundamental aspect. One such study by (Ronconi et al., 2016) examined the neural basis of visual crowding, utilizing EEG to measure event-related potentials and oscillatory dynamics. EEG offers a temporal resolution

on the scale of milliseconds, enabling researchers to accurately track the timing of activation across the visual hierarchy while studying visual crowding. For this reason, this technique can provide valuable insights into the neural substrates associated with visual crowding. In this study, visual crowding of complex objects (such as letters) in the peripheral visual field was manipulated by varying the critical spacing between the target and the flankers, while carefully controlling for changes in the physical properties of the stimulus array. Using dense-array EEG the authors aimed to determine whether visual crowding for complex objects like letters occurs at an early or late stage of visual processing. Additionally, they examined event-related oscillatory responses in the alpha (8-12 Hz), beta (15-30 Hz), and gamma (30-80 Hz) frequency ranges, which had not previously been explored in relation to visual crowding. The behavioral results matched the authors' hypotheses precisely: the strong crowding condition showed lower accuracy compared to both the mid crowding and no crowding conditions. Additionally, the mid crowding condition demonstrated lower accuracy compared to the no crowding condition. The ERPs results indicated that the first sign of crowding-induced modulation in EEG activity was the suppression of the N1 component. This finding aligns with the evidence from Chicherov et al. (2014), which also demonstrated that the earliest marker of visual crowding was N1 component suppression. Consistently, earlier studies on texture segmentation (Bach & Meigen, 1997; Caputo & Casco, 1999; Fahle et al., 2003) and contour detection (Machilsen & Wagemans, 2011; Mathes et al., 2006; Shpaner et al., 2013) have generally found that N1 suppression is associated with the inability to segment a stimulus target from its background. Moreover, these studies have shown that the N1 component reflects activation in higher-level areas (Murray et al., 2002; Pei et al., 2005.; Shpaner et al., 2013), supporting the idea that crowding is a late-stage process. The analysis of oscillatory activity further confirmed that visual crowding is associated with neural processing at a later stage in the visual hierarchy. A reduction in power within the beta band (15-30 Hz) reflected the level of visual crowding. Specifically, the strong crowding condition showed a greater reduction in beta band activity compared to the mid crowding condition, beginning around 200 milliseconds after the stimulus onset. Moreover, the suppression of beta activity as marker of visual crowding was supported by the observation that greater suppression following stimulus onset was linked to behavioral performance more impacted by visual crowding. In conclusion, this study modulated visual crowding of complex objects (such as letters) and found that differences related to crowding became apparent through the suppression of the N1 ERP component and a reduction in beta power, both occurring within similar time frames. These results support the idea that

crowding, particularly for complex visual stimuli, arises at later stages of the visual processing hierarchy and highlight the important role of beta frequency in this phenomenon.

After the study just discussed (Ronconi et al., 2016), the authors decided to conduct single-trial analyses of EEG oscillations to assess the prestimulus power and phase differences between correct and incorrect discriminations in a letter-crowding task, where irrelevant letters were positioned either close to (strong crowding) or farther from (mid crowding) the target (Ronconi & Bellacosa Marotti, 2017). The main novelty of this study is that the authors focus on pre-stimulus activity. In fact, direct attempts to find neural correlates of visual crowding up to this point have primarily focused on investigating post-stimulus activity. While in this case the authors aimed to explore the brain states that facilitate accurate perception under different crowding conditions. To achieve this, they used high-temporal resolution techniques like EEG to measure neural oscillations occurring before the onset of the target stimulus. In other words, they sought to identify which properties of these ongoing oscillations could predict the accurate perception of visual stimuli in a crowded environment. They found that pre-stimulus oscillatory power (i.e., amplitude) in the beta band (13–20 Hz) predicted accurate object perception in the strong crowding condition, but not in the mid crowding condition. This effect was reflected in higher beta power during accurate trials across a large cluster of parieto-occipital sensors, in a time window just before stimulus onset. The authors suggest that increased beta power in parieto-occipital channels prior to stimulus onset may prime the visual system for the local processing needed to distinguish a stimulus within a crowded scene. In conclusion, this study explored the prestimulus electrophysiological markers that predict a complete conscious representation of visual objects under varying crowding conditions. Their findings indicate that, just before stimulus onset, the visual system's predisposition to extract local information plays a significant role, as evidenced by the modulation of beta power in parieto-occipital channels.

Building on the findings from the two previously discussed studies (Ronconi et al., 2016; Ronconi & Bellacosa Marotti, 2017), which showed a connection between visual crowding and EEG oscillations in the beta band (15–30 Hz), Battaglini et al. (2020) aimed to test the hypothesis of a causal relationship between visual crowding and beta band power. Since establishing a causal relationship requires directly modulating these neural oscillations, and transcranial alternating current stimulation (tACS) is a suitable method for this purpose, the authors employed tACS to test their hypothesis. They specifically hypothesized that applying tACS over the right parietal cortex at the beta frequency (18 Hz) would enhance

performance in a visual crowding task compared to a control frequency (10 Hz) or a no-stimulation (sham) condition. This hypothesis was tested using a classic crowded letter orientation discrimination paradigm. Additionally, to determine whether tACS could induce changes in endogenous brain rhythms (Helfrich et al., 2014), they recorded resting-state EEG signals to measure power differences in the relevant frequency bands (beta and alpha) before and after stimulation. The results demonstrated a lower threshold for stimuli presented in the contralateral hemifield when participants received 18-Hz tACS over the right parietal cortex, compared to 10-Hz tACS and sham stimulation at the same cortical site. These findings support the previously reported connection between beta frequency activity in the parietal cortex and visual crowding (Ronconi et al., 2016; Ronconi & Bellacosa Marotti, 2017). Additionally, EEG recordings revealed that parietal tACS at beta frequency not only influences behavior but also significantly alters endogenous oscillatory dynamics. This suggests that the efficiency of the right dorsal fronto-parietal network can be modulated by tACS at specific frequencies. These findings provide the first evidence that visual crowding can be reduced by applying beta neurostimulation to the parietal region.

These findings were further supported by a later study (Di Dona et al., 2024). Building on their previous research (Battaglini et al., 2020), they aimed to clarify the distinct functional roles of beta oscillations in the parietal cortices and the right fronto-parietal network during visual crowding. Specifically, they investigated whether the improvements in reducing the effects of visual crowding through right parietal stimulation, as found by Battaglini et al. (2020), and which were previously limited to the contralateral visual hemifield, could be extended to both visual hemifields. They hypothesized that by applying electrical stimulation to both parietal cortices, the positive effects on visual performance would extend across the entire visual field. The study's behavioral finding was a lower threshold for letter orientation discrimination when 18 Hz tACS was applied to both parietal cortices, compared to when the same stimulation was applied to the right fronto-parietal network or when no stimulation was given. In summary, they found that bilateral parietal beta tACS reduces the effects of visual crowding across the entire visual field. These results support the functional predominance of beta oscillations over the parietal cortices, aligning with previous studies that describe beta as the "natural" rhythm of parietal regions (Cabral-Calderin & Wilke, 2020; Capilla et al., 2022; Samaha et al., 2017). Furthermore, they reinforce earlier findings on the critical role of parietal beta oscillations in visual crowding (Battaglini et al., 2020; Ronconi et al., 2016; Ronconi & Bellacosa Marotti, 2017). These findings are also consistent with the

idea that crowding results from incorrect integration of target and flanker features (Parkes et al., 2001; Pelli, 2008), which is supported by a dorsal-to-ventral projection originating from parietal areas.

While the previously mentioned studies (Battaglini et al., 2020; Di Dona et al., 2024) found that beta-frequency tACS stimulation on the parietal region of the brain seems to enhance perception, namely the ability to segment the target from distractors, in visual crowding situations, a study by Stonkus et al. (2016) suggests that theta-frequency tACS stimulation (7 Hz) could potentially improve performance in a perceptual integration task. The authors used brief event-related transcranial alternating current stimulation (tACS) to selectively modulate prestimulus 7 Hz oscillations (theta frequency band) and the synchrony between parietal and occipital brain regions. Their aim was to test the causal role of these specific prestimulus oscillations in perceptual integration, which involves transforming distributed activity in lower visual regions into meaningful object representations by integrating neural information across object features (Robertson, 2003) or across space (Roelfsema, 2006). This process includes bottom-up signaling of candidate features into a spatial map (Tootell et al., 1998), as well as top-down selection of targets based on spatial location (Foxe & Snyder, 2011). Therefore, perceptual integration depends on communication between cortices at different levels of the visual processing hierarchy, specifically in the occipital and parietal regions. Additionally, the authors recorded EEG simultaneously to examine frequency-specific aftereffects. Their results demonstrated a significant main effect of stimulation on perceptual integration, with in-phase 7 Hz stimulation leading to the highest performance levels. Furthermore, electrophysiological findings suggest that brief tACS induces oscillatory entrainment, as indicated by the registration of frequency-specific aftereffects.

Building on this evidence, in this study, we aim to modulate the strength of the Delboeuf illusion using different tACS stimulation frequencies. Indeed, the Delboeuf illusion requires processing both the central element (or squares) and the surrounding background. Therefore, we can hypothesize that if tACS can influence the perceptual ability to integrate or segregate elements in an image using different frequencies, it might also be possible to modulate the strength of the Delboeuf illusion. If tACS at various frequencies affects the strength of both the classical (same area shown in different contexts) and numerical (same numerosity presented in different contexts) versions of the Delboeuf illusion in a similar manner and to the same extent, this would further support the hypothesis of a generalized

magnitude system in humans. Specifically, each participant was tested three times, with a different type of neural stimulation each time (7 Hz, 18 Hz, and no stimulation), and was exposed to both types of the Delboeuf illusion during each session. We hypothesize that theta-band stimulation (7 Hz) over the right parietal area will enhance the integration of visual elements into a global percept, thereby intensifying the illusion compared to the no stimulation (sham) condition. On the other hand, beta-band stimulation (18 Hz) over both the right and left parietal lobes is expected to promote the segregation of visual elements, reducing the illusion's strength compared to the sham condition.

Materials and methods

Ethics statements

The study was approved on the 11th of April 2023 by the ethics committee (Protocol no. 5179, code no. 766656C6F2B60F2D3731E72418CD558B) of the Department of General Psychology at the University of Padova (Italy). Data collection was done between 23 May 2023 and 24 July 2023.

Participants

In this study, we recruited 48 adult volunteers (38 females and 10 males; mean age ± SD = 24.19 ± 3.02 years), all of whom were students at the University of Padova enrolled in either bachelor's or master's programs. All participants reported having normal or corrected-to-normal vision. Eligibility for transcranial electrical stimulation was determined through a pre-screening test at the start of each session. Exclusion criteria included neurological disorders that affect visual and/or numerical abilities, substance abuse, and any medical conditions that could pose a risk to participants (e.g., pacemaker, epilepsy, migraine auras). Some participants did not meet the criteria for receiving tACS and were therefore excluded from the study. As a result, the final sample included 34 participants (age range: 21-35 years, with 5 males). At the end of each session, a post-stimulation questionnaire was administered to assess participants' well-being and to determine whether they believed they had received actual stimulation or a sham condition (i.e., placebo; see Fertonani et al., 2015). Before participating in the experiment, all participants provided informed consent in accordance with the Declaration of Helsinki.

Experimental set-up and tACS stimulation

The study was carried out in a dimly lit room to minimize the detection of phosphenes induced by transcranial electrical stimulation (tES) (Evans et al., 2022). Participants were asked to use a chin rest positioned 57 cm from the monitor. The stimuli were presented on an ASUS LCD monitor with a resolution of 1280 × 1024 and a refresh rate of 60Hz. tACS was administered over the parietal areas using a BrainSTIM device (E.M.S. srl) at an intensity of 1 mA. Carbonised rubber electrodes, measuring 5 × 5 cm and covered in sponges, were placed at the locations corresponding to P3 and P4 on a 64-channel EEG cap arranged according to the international 10-20 system. In the active conditions, the

current was applied for 45 min (with 10-s fade-in and -out periods at the stimulation's beginning and end). In the sham tACS, the current was turned off 10 s after the beginning of the stimulation (with 10-s fade-in and -out periods, for a total of 30 s). The majority of the participants reported experiencing absence or low level of fatigue during the test, independently on the stimulation type ($\chi^2_9 = 8.14$, $p = 0.52$). No phosphenes were reported. Moreover, they were not able to discriminate between real stimulation and placebo, as confirmed by a Pearson's Chi-Square test for frequency distribution ($\chi^2_1 = 1.76$, $p = 0.18$; the observed probability of reported "stimulation present" was 0.60 in the 7Hz tACS condition, 0.52 in the 18Hz tACS condition and 0.75 in the sham condition). Stimulation parameters were selected in accordance with the safety guidelines provided by Antal et al. (2017).

Stimuli

We employed two different types of stimuli. For numerical discrimination, the stimuli were composed of two arrays of orange squares positioned within two white circular backgrounds, which were placed inside two black rectangles (Figure 8). For continuous quantity discrimination, the stimuli consisted of two orange circles within two white circular backgrounds, also enclosed within 4.5 × 4.5 cm black rectangles, similar to the setup for the numerical discrimination task (Figure 8). For each type of discrimination, we organized two types of trials: control trials and illusory trials. In control trials, there was an actual difference between the two stimuli: for numerical discrimination, one stimulus had 10 squares and the other had 12 squares (a ratio of 0.83). For continuous quantity discrimination, the areas of the circles differed by the same ratio as in the numerical discrimination. For the control trials, four different combinations of numerosity or circles and backgrounds were used, following the approach of a previous study by Santacà & Granziol (2023). In "large trials", the two target stimuli to discriminate were presented in two identical large backgrounds (4.22 cm in diameter; Figure 8a). Conversely, in "small trials", the two target stimuli were presented in two identical small backgrounds (2.79 cm in diameter; Figure 8b). In the remaining two types of trials, different backgrounds were utilized within each pair of stimuli. In "congruent trials", the larger target stimulus was presented in the large background and the smaller stimulus in the small background (2.79 cm and 4.22 cm in diameter; Figure 8c). In "incongruent trials", the large background included the smaller stimulus, and the small background surrounded the larger stimulus (2.79 cm and 4.22 cm in diameter; Figure 8d). Lastly, illusory trials consisted of the same numerosity or the same circles in two different backgrounds, a large

and a small one (2.79 cm and 4.22 cm in diameter; Figure 8e), resembling the numerical or classical Delboeuf illusion respectively. For numerical discrimination, we created six different pairs for both control and illusory trials, where both the position and size of the squares varied. The side lengths of the squares ranged from 0.15 cm to 0.30 cm. Similarly, for continuous quantity discrimination, we arranged six different pairs for both control and illusory trials, where the diameters of the circles varied between 1.64 cm and 2.35 cm.

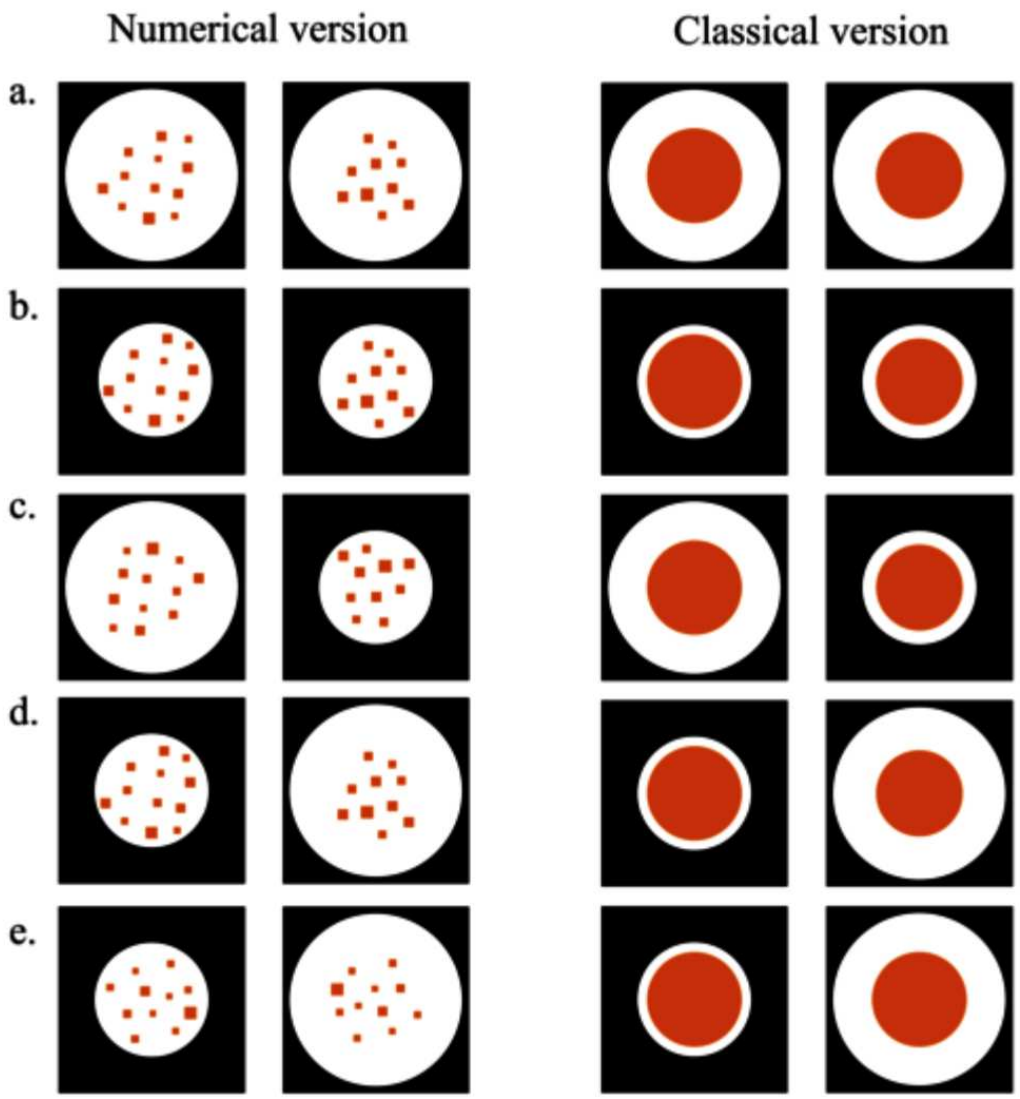

Figure 8. The figure shows an example of the four types of control trials for both discriminations: a large trial (a), a small trial (b), a congruent trial (c) and an incongruent trial (d). The figure also shows an example of illusory trial (e), in which the same numerosity/same target circle is presented in two different-sized backgrounds resembling the Delboeuf illusion.

As detailed in a previous study by Santacà & Granziol (2023), a key challenge in assessing numerical discrimination is that numerosity often varies alongside other physical properties

of the stimuli, referred to as non-numerical continuous variables. These variables include the cumulative surface area (the total area covered by all elements of a stimulus), the size of the elements, the overall space occupied by the elements, and their density. These non-numerical continuous variables are carefully controlled in numerical cognition studies because participants might rely on these cues to judge which array has a larger or smaller numerosity (e.g., Gebuis & Reynvoet, 2012; Vos et al., 1988). To avoid this, control trials ensured that pairs of stimuli were matched for cumulative surface area. However, matching the cumulative surface area can result in smaller-than-average squares appearing more frequently in arrays with higher numerosities, which participants might use as a cue instead of the actual number. To minimize this, the ratio of the cumulative surface area of the smaller numerosity to the larger numerosity was adjusted to be between 76-85% for one-third of the stimuli, 86-95% for another third, and 96-105% for the final third, following the approach of previous studies (e.g., Bisazza et al., 2014; Miletto Petrazzini & Brennan, 2020). Furthermore, given the negative correlation between density and the overall space occupied by the squares, half of the pairs in each discrimination task were controlled for density, while the other half were controlled for the overall space occupied by the squares. In illusory trials, the same target stimulus was used for each pair to prevent participants from making decisions based on other physical characteristics, such as cumulative surface area, element size, overall space occupied, or density. Thus, the performance in the illusory trials would solely indicate the direct effect of the Delboeuf illusion on numerosity estimation, without any indirect influence from a biased perception of convex hull, occupied area, or density. Additionally, to reduce the chance that participants would notice that the squares in the two illusory arrays were identical in size and position, each numerosity array was rotated in every illusory trial. The two arrays were displayed in the left-center and right-center quadrants of the computer screen.

Procedure

Each experimental session was divided into two blocks: one block involved numerical stimuli, while the other involved the other type of stimuli (continuous quantity, namely circles). Each block consisted of 300 trials and lasted about 20 minutes, with a 5-minute break in between, making the total duration of the experimental session around 45 minutes. Participants received both oral and written instructions before the experiment began.

During the experimental session, participants were shown pairs of stimuli of the same type (either numerical or continuous quantity discrimination) that were positioned 8 cm apart. They were instructed to use a QWERTY keyboard to indicate which stimulus appeared more numerous or larger, depending on the type of discrimination task. Specifically, participants pressed the "S" key to select the stimulus on the left side of the screen and the "L" key for the stimulus on the right. The order of the two blocks, as well as the different trial types within each block, was randomized for each participant. At the start of each block, a fixation cross appeared in the center of the screen for 250 ms. Participants were instructed to keep their gaze focused on the center of the monitor throughout the block. The paired stimuli were presented for 150 ms, a duration short enough to prevent saccadic eye movements toward the target or verbal counting during numerical discrimination. After the stimuli disappeared, a white screen was displayed for 550 ms, during which participants were required to make their choice. If they did not respond within this period, the trial was considered invalid. The experiment included three sessions for each participant, conducted on non-consecutive days with at least 48 hours between sessions. In each session, participants completed both discrimination tasks but under different stimulation conditions. Specifically, participants experienced a sham condition with no stimulation and two active conditions with stimulation at different frequencies: 7 Hz and 18 Hz tACS. The order of these stimulation conditions was randomized across sessions so that each participant experienced all conditions but in a different sequence.

Statistical analyses

Data were analyzed in R version 3.5.2 (R Core Team. R, 2016). For all three stimulations (7Hz, 18Hz, sham), we recorded accuracy in terms of selecting the larger target stimulus and numerosity for control trials. In illusory trials, we scored as ‘correct’ the choices for the stimulus and the numerosity presented in the small context. At the individual level, we used binomial tests to compare the choices for the larger target stimulus and numerosity in control trials and for the stimulus and the numerosity presented in the small context in illusory trials (chance level = 0.5). We performed group analyses on the frequency of choices for the larger target stimulus and numerosity in control trials and for the stimulus and the numerosity presented in the small context in illusory trials. Not all data were normally distributed (Shapiro–Wilk test, $p<0.05$); thus, we performed one-sample t tests or Wilcoxon-signed rank tests (chance level = 0.5).

Considering only the sham condition, a Pearson correlation test was performed to assess the correlation between the performances of the two discriminations (numerical vs. continuous quantity discrimination) both considering only those control trials in which the Delboeuf illusion has no effect (small and large trails) and only those trials in which the illusion should have an effect (congruent trials, incongruent trials, illusory trials).

We also assessed the accuracy of responses by fitting a generalized mixed-effects model for binomial distributions (GLMM) with three within variables: the stimulation (7 Hz, 18 Hz or sham), the discrimination (numerical or continuous quantity), and the stimulus type (large, small, congruent, incongruent or illusory trials). We fitted each of these variables, as well as their two- and three way interactions, as fixed effects whereas we fitted subjects as clustering variable and random factor (i.e., random intercept model). Sum contrasts were set for the three abovementioned predictors. GLMMs were estimated with a Maximum Likelihood (Laplace Approximation) procedure with the function glmer() from the lme4 package (Bates et al., 2015). Whenever a main effect emerged as statistically significant (the Anova() function of the car package was used; (Fox et al., 2012)), post-hoc comparisons were performed with the function emmeans() from the emmeans package (Lenth, 2023). Considering the number of comparisons that could arise from high-order effects such as interactions, not all the comparisons were analyzed. In particular when examining the interaction between stimulus and task we analyzed only the difference between stimulus type for each task type (see Table 2). In this way, it was reduced the chance of committing Type I error due to comparisons that were beyond the aim of the present work. Nonetheless, the False Discovery rate method (Benjamini & Hochberg, 1995) was used to adjust post-hoc comparisons. For each comparison, Odds Ratios (ORs), their 95% confidence intervals (CI), statistics (z), standard error (SE), p-values (p) are also reported. As suggested by several works (Harris, 2021; Lenzi et al., 2015), when reporting OR, the outcomes may be presented in two different formats: as a percentage difference in likelihood, which is calculated by subtracting the Odds Ratios from 1.0, and as “n times less/more likely”, which is determined by dividing 1.0 by the OR in the former case (i.e., “less”). In the present paper, the latter way was preferred, since ORs below 1.0 may be less straightforward and intuitive for interpreting the strength of associations compared to ORs above 1.0. Overall, three different GLMMs were performed: two models tested the interaction between the stimulus type and the stimulation only in the numerical discrimination or only in the continuous quantity discrimination. Lastly, we performed an overall model including the discrimination

type with the two former predictors (See Figure S1, Supplementary Material, for a schematization of the analyses that have been described).

In preparation for a future study, we also decided to use the knowledge learned in this study to perform a power analysis. Specifically, we performed a power analysis using the parameters of the GLMM we fitted to predict the sample size needed to have sufficient power (i.e. probability that the test will reject the null hypothesis, assuming that the null hypothesis is false). In particular, we tested the interaction effect between the Stimulus factor and the Stimulation factor. The predicted effect size for this effect, which was used for the power analysis, is the one identified in this study and alpha was kept at 0.05. To perform this analysis we used the R package simr (Green & MacLeod, 2016), which allows users to calculate power for generalized linear mixed models from the lme4 package. These power calculations are performed using Monte Carlo simulations. Specifically, we used the powercurve() function to generate power curves, which help evaluate the trade-offs between power and sample size. Here is how a power analysis works in simr. The following steps are each repeated n times (number of simulation, for this study 1000 which is the default option in simr): (1) simulate a new set of data based on the provided fitted model, (2) refit the model to this newly simulated data, and (3) conduct a statistical test on the refitted model. The test will either successfully detect the effect or make a Type II error in failing to detect the effect. The power of the test is then determined by the proportion of times the effect is successfully detected in step three.

Results

Behavioral level: sham condition

Numerical discrimination

For the numerical discrimination, individual analyses revealed that 23 out of 34 participants selected the larger numerosity significantly more than chance in control trials (mean ± SD = 61.00 ± 9.16 %; Table S1, Supplementary Material). Considering the Delboeuf illusory trials, 9 out of 34 participants selected the numerosity presented in the small context significantly more than chance whereas, interestingly, 5 selected more than chance the one presented in the large context (mean ± SD = 54.51 ± 16.51 %; Table S1, Supplementary Material).

Group analyses revealed that participants selected the larger numerosity significantly more than chance in control trials (mean ± SD = 62.35 ± 8.30 %; Wilcoxon-signed rank test, Z = 0.98, $p < 0.001$*). Overall, participants did not perceive the numerical Delboeuf illusion, since they did not select any numerosity significantly more than chance (mean ± SD = 54.51 ± 16.85 %; one-sample *t* test, $t_{33} = 1.56$, $p = 0.128$).

Continuous quantity discrimination

Individual analyses revealed that 23 out of 34 participants selected the larger target stimulus significantly more than chance in control trials (Table S1, Supplementary Material). Considering the Delboeuf illusory trials, 27 out of 34 participants selected the stimulus presented in the small context significantly more than chance (Table S1, Supplementary Material).

Group analyses revealed that participants selected the larger target stimulus significantly more than chance in control trials (mean ± SD = 62.35 ± 8.30 %; Wilcoxon-signed rank test, Z = 1.07, $p < 0.001$*). Participants also proved to perceive the Delboeuf illusion as expected, so selecting the stimulus presented in the small context significantly more than chance (mean ± SD = 80.38 ± 17.70 %; Z = 1.10, $p < 0.001$*).

Correlation between numerical and continuous quantity discrimination

Considering only those control trials in which the Delboeuf illusion has no effect, we found a significant correlation between performance in the two discriminations (Pearson correlation; $r_{34} = 0.37$, $p = 0.032$). Even considering only those trials in which the illusion has an effect, we found a significant correlation between performance in the two discriminations (Pearson correlation; $r_{34} = 0.38$, $p = 0.029$). The first correlation suggests that those participants who have a higher discrimination ability with continuous quantities also better discriminate between different numerosities. The second correlation instead suggests that those participants who are more influenced by the Delboeuf illusion when it is resembled with a continuous quantity, are also more influenced by it when it is resembled with numerosity arrays.

Neural level: 7 Hz and 18 Hz tACS stimulations

Numerical discrimination

In the 7 Hz tACS stimulation, individual analyses revealed that 17 out of 34 participants selected the larger numerosity significantly more than chance in control trials (Table S1, Supplementary Material). Considering the Delboeuf illusory trials, 12 out of 34 participants selected the numerosity presented in the small context significantly more than chance whereas, interestingly, 4 selected more than chance the one presented in the large context (Table S1, Supplementary Material).

Group analyses revealed that, in the 7 Hz tACS stimulation, participants selected the larger numerosity significantly more than chance in control trials (mean ± SD = 58.88 ± 8.58 %; one-sample *t* test, $t_{33} = 6.21$, $p < 0.001$*). Overall, participants proved to perceive the numerical Delboeuf illusion, so selecting the numerosity presented in the small context significantly more than chance (mean ± SD = 57.88 ± 18.88 %; $t_{33} = 2.43$, $p = 0.021$*).

In the 18 Hz tACS stimulation, individual analyses revealed that 18 out of 34 participants selected the larger numerosity significantly more than chance in control trials (Table S1, Supplementary Material). Considering the Delboeuf illusory trials, 10 out of 34 participants selected the numerosity presented in the small context significantly more than chance whereas, interestingly, 4 selected more than chance the one presented in the large context (Table S1, Supplementary Material).

Group analyses revealed that, in the 18 Hz tACS stimulation, participants selected the larger numerosity significantly more than chance in control trials (mean ± SD = 59.59 ± 8.69 %; one-sample *t* test, t_{33} = 6.289, p < 0.001*). Overall, participants did not perceive the numerical Delboeuf illusion, since they did not select any numerosity significantly more than chance (mean ± SD = 55.55 ± 16.59 %; t_{33} = 1.951, p = 0.060).

Considering the GLMM, it was not observed a statistically significant effect of the stimulation on the participants' accuracy (χ^2_2 = 4.11, p = 0.128). On the other hand, a statistically significant effect of the trial type emerged (χ^2_4 = 248.58, p < 0.001). In detail, participants reported a significantly lower accuracy in congruent trials, compared to the other trial type (all p < 0.001). In the case of incongruent trials, the accuracy was significantly higher, compared to the other trial type (all p < 0.05). In the case of large trials, the accuracy was higher, especially when compared to both small (p < 0.001) and illusory trials (p < 0.001). With small trials, the accuracy tended to be lower, compared to illusory trials (p < .001). The complete list of these post-hoc comparisons, including ORs, their 95% CI, *z*-values, SE, and *p*-values can be found in Table 2. Lastly, considering the interaction among the stimulation and the trial type, no statistically significant effect was found (χ^2_8 = 9.16, p = 0.329).

Continuous quantity discrimination

In the 7 Hz stimulation, individual analyses revealed that 26 out of 34 participants selected the larger target stimulus significantly more than chance in control trials (Table S1, Supplementary Material). Considering the Delboeuf illusory trials, 29 out of 34 participants selected the stimulus presented in the small context significantly more than chance (Table S1, Supplementary Material).

Group analyses revealed that, in the 7 Hz tACS stimulation, participants selected the larger target stimulus significantly more than chance in control trials (mean ± SD = 61.58 ± 7.40 %; Wilcoxon-signed rank test, Z = 1.08, p < 0.001*). Participants also proved to perceive the Delboeuf illusion, so selecting the stimulus presented in the small context significantly more than chance (mean ± SD = 78.81 ± 18.44 %; Z = 1.07, p < 0.001*).

In the 18 Hz tACS stimulation, individual analyses revealed that 28 out of 34 participants selected the larger target stimulus significantly more than chance in control trials (Table S1, Supplementary Material). Considering the Delboeuf illusory trials, 29 out of 34 participants

selected the stimulus presented in the small context significantly more than chance (Table S1, Supplementary Material).

Group analyses revealed that, in the 18 Hz tACS stimulation, participants selected the larger target stimulus significantly more than chance in control trials (mean ± SD = 63.00 ± 6.98 %; Z = 1.159, $p < 0.001$*). Participants also proved to perceive the Delboeuf illusion, so selecting the stimulus presented in the small context significantly more than chance (mean ± SD = 82.05 ± 17.93 %; Z = 1.097, $p < 0.001$*).

Considering the GLMM, a statistically significant effect of the stimulation on the participants' accuracy was found ($\chi^2_2 = 9.52$, $p = 0.009$): participants were more likely to correctly respond in case of the 18 Hz tACS stimulation, compared to the 7 Hz tACS stimulation ($p < 0.01$); comparing both 18 Hz and 7 Hz tACS stimulations with the sham condition, no differences in accuracy emerged ($p > 0.05$). Concerning the trial type, a statistically significant effect emerged ($\chi^2_4 = 4437.38$, $p < 0.001$). In detail, compared to all the other trials, the accuracy on congruent trials was lower (all $p < 0.001$), as also found for the numerical discrimination. With incongruent trials, the accuracy was higher (all $p < 0.001$), compared to all the other trial types as also found for the numerical discrimination. The performances in both large and small trials were not significantly different ($p = 0.273$). Instead, in illusory trials, the accuracy was significantly higher, compared to both large ($p < 0.001$) and small trials ($p < 0.001$). The complete list of these post-hoc comparisons, including ORs, their 95% CI, *z*-values, SE, and *p*-values can be found in Table 2. Lastly, considering the interaction between the stimulation and the trial type, no statistically significant effect was found ($\chi^2_8 = 5.78$, $p = 0.672$).

Comparison between numerical and continuous quantity discrimination

In the overall model, the effect of the discrimination emerged as statistically significant ($\chi^2_1 = 443.75$, $p < 0.001$). In particular, participants were significantly more accurate in the continuous quantity discrimination than the numerical one ($p < 0.001$). Furthermore, a statistically significant effect of the stimulation was observed ($\chi^2_2 = 8.79$, $p = 0.012$): participants were less likely to respond correctly in case of the 7 Hz tACS stimulation both compared to the 18 Hz tACS stimulation ($p = 0.019$) and to the sham condition ($p = 0.028$). No difference in accuracy was found between the 18 Hz tACS stimulation and the sham condition ($p = 0.698$). Considering the interaction between discrimination and stimulation,

no statistically significant effect was found ($\chi^2_2 = 5.56$, $p = 0.062$, Figure S2, Supplementary Materials).

Considering the trial type, a statistically significant effect was observed ($\chi^2_4 = 3352.26$, $p < 0.001$). As for the previous models, the accuracy in congruent trials was lower, compared to all the other types of trials (all $p < 0.001$). On the other hand, in incongruent trials, the accuracy was higher compared to all the other trial types (all $p < 0.001$). Instead in the large trials, participants were more likely to respond correctly compared to small trials ($p < 0.001$). In illusory trials, the accuracy was higher, compared to both large ($p < 0.001$) and small trials ($p < 0.001$).

The interaction between the discrimination and the trial type emerged as a statistically significant ($\chi^2_4 = 1930.38$, $p < 0.001$). In the continuous quantity discrimination, all the previous differences among trial types were found. The only exception concerned the difference in accuracy between large and small trials, that emerged to be no longer statistically significant ($p = 0.277$, Figure 9). In the numerical discrimination, the direction of some differences changed: contrary to the results of the trial type main effect, in the case of large trials, participants were more likely to respond correctly compared to both small ($p < 0.001$) and illusory trials ($p < 0.001$); finally, in the case of small trials, participants were more likely to respond correctly compared to illusory trials ($p < 0.001$). All the other comparisons were statistically significant and coherent with the previous main effects (see Table 2). No further statistically significant effects emerged (all $p > 0.05$).

Power analysis

The results of the power analysis indicated that, with the parameters we specified, a numerosity of 45 subjects in a future study would lead us to a predicted power (95% confidence interval) of 83.20% (80.74 , 85.47) for the test of the interaction between the Stimulus and the Stimulation (Figure 10). While a numerosity of 50 subjects would lead us to a predicted power (95% confidence interval) of 87.60% (85.40 , 89.58).

Table 2. Post-hoc comparisons of all the GLMMs.

	Comparison	OR	Lower CI	Upper CI	SE	*z*	*p* adjusted
Model on numerical discrimination	congruent / incongruent	0.600	0.539	0.667	0.023	-13.524	< 0.001 *
	congruent / large	0.655	0.590	0.728	0.025	-11.245	< 0.001 *
	congruent / small	0.759	0.684	0.842	0.028	-7.411	< 0.001 *
	congruent / illusion	0.887	0.799	0.984	0.033	-3.233	0.001 *
	incongruent / large	1.093	0.981	1.217	0.042	2.312	0.021 *
	incongruent / small	1.265	1.137	1.408	0.048	6.181	< 0.001 *
	incongruent / illusion	1.479	1.330	1.645	0.056	10.328	< 0.001 *
	large / small	1.158	1.041	1.287	0.044	3.872	< 0.001 *
	large / illusion	1.353	1.218	1.504	0.051	8.035	< 0.001 *
	small / illusion	1.169	1.053	1.298	0.044	4.180	< 0.001 *
Model on continuous quantity discrimination	congruent / incongruent	0.068	0.060	0.078	0.003	-57.449	< 0.001 *
	congruent / large	0.182	0.162	0.204	0.007	-41.927	< 0.001 *
	congruent / small	0.190	0.169	0.213	0.008	-41.084	< 0.001 *
	congruent / illusion	0.092	0.082	0.105	0.004	-53.858	< 0.001 *
	incongruent / large	2.668	2.344	3.037	0.123	21.283	< 0.001 *
	incongruent / small	2.787	2.450	3.171	0.128	22.322	< 0.001 *
	incongruent / illusion	1.356	1.181	1.556	0.067	6.197	< 0.001 *
	large / small	1.045	0.934	1.168	0.042	1.096	0.273
	large / illusion	0.508	0.450	0.574	0.022	-15.531	< 0.001 *

	small / illusion	0.486	0.431	0.549	0.021	-16.611	< 0.001 *
	18 hz / 7 hz	1.111	1.024	1.206	0.038	3.080	< 0.01 *
	18 hz / control	1.061	0.978	1.152	0.036	1.732	0.125
	7 hz / control	0.955	0.881	1.035	0.032	-1.363	0.173
Overall model: comparison between numerical and continuous quantity discrimination	congruent / incongruent	0.206	0.189	0.224	0.006	-52.897	< 0.001 *
	congruent / large	0.349	0.323	0.377	0.010	-38.104	< 0.001 *
	congruent / small	0.384	0.356	0.415	0.011	-34.937	< 0.001 *
	congruent / illusion	0.291	0.268	0.315	0.008	-43.033	< 0.001 *
	incongruent / large	1.697	1.56	1.846	0.051	17.671	< 0.001 *
	incongruent / small	1.867	1.718	2.030	0.056	20.999	< 0.001 *
	incongruent / illusion	1.414	1.296	1.542	0.044	11.200	< 0.001 *
	large / small	1.100	1.019	1.188	0.030	3.483	< 0.001 *
	large / illusion	0.833	0.769	0.903	0.024	-6.350	< 0.001 *
	small / illusion	0.757	0.699	0.820	0.022	-9.745	< 0.001 *
	18 Hz / 7 Hz	1.063	1.008	1.122	0.024	2.729	0.019 *
	18 Hz / control	1.009	0.956	1.065	0.023	0.388	0.698
	7 Hz / control	0.949	0.900	1.001	0.021	-2.358	0.028 *
	Continuous quantity / numerical discrimination	1.469	1.418	1.523	0.027	21.065	< 0.001 *
	Continuous quantity: congruent / incongruent	0.071	0.062	0.081	0.003	-57.23	< 0.001 *
	Continuous quantity:	0.187	0.165	0.211	0.008	-41.701	< 0.001 *

congruent / large						
Continuous quantity: congruent / small	0.195	0.173	0.220	0.008	-40.802	< 0.001 *
Continuous quantity: congruent / illusion	0.096	0.084	0.109	0.004	-53.69	< 0.001 *
Continuous quantity: incongruent / large	2.636	2.295	3.028	0.121	21.162	< 0.001 *
Continuous quantity: incongruent / small	2.752	2.398	3.159	0.126	22.194	< 0.001 *
Continuous quantity: incongruent / illusion	1.351	1.165	1.566	0.066	6.159	< 0.001 *
Continuous quantity: large / small	1.044	0.926	1.177	0.041	1.088	0.277
Continuous quantity: large / illusion	0.512	0.450	0.584	0.022	-15.462	< 0.001 *
Continuous quantity: small / illusion	0.491	0.431	0.559	0.021	-16.513	< 0.001 *
Numerical: congruent / incongruent	0.599	0.534	0.671	0.023	-13.537	< 0.001 *
Numerical: congruent / large	0.654	0.584	0.733	0.025	-11.27	< 0.001 *
Numerical: congruent / small	0.758	0.677	0.849	0.028	-7.408	< 0.001 *
Numerical:	0.886	0.792	0.991	0.033	-3.255	0.001 *

congruent / illusion						
Numerical: incongruent / large	1.093	0.973	1.227	0.042	2.303	0.022 *
Numerical: incongruent / small	1.267	1.129	1.421	0.048	6.208	< 0.001 *
Numerical: incongruent / illusion	1.480	1.320	1.660	0.056	10.332	< 0.001 *
Numerical: large / small	1.159	1.034	1.300	0.044	3.902	< 0.001 *
Numerical: large / illusion	1.355	1.209	1.519	0.051	8.051	< 0.001 *
Numerical: small / illusion	1.169	1.044	1.308	0.044	4.166	< 0.001 *

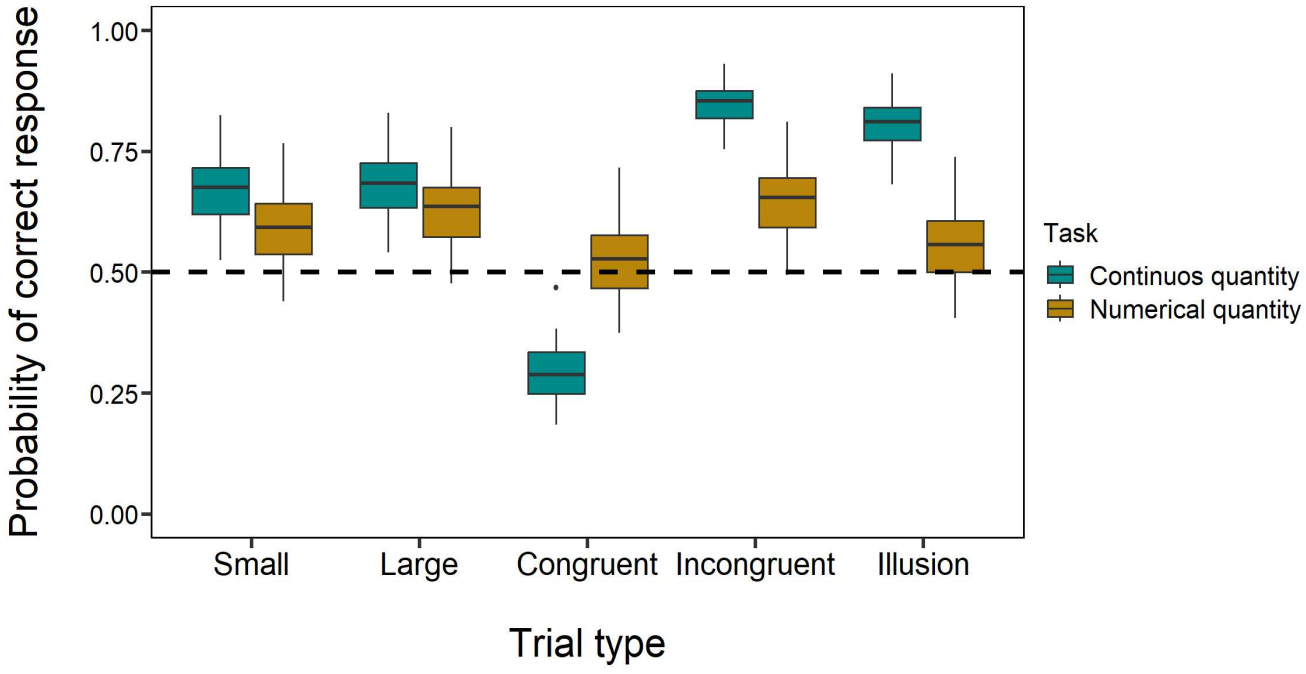

Figure 9. Comparison of the performances in the two discrimination tasks in all five types of trials.

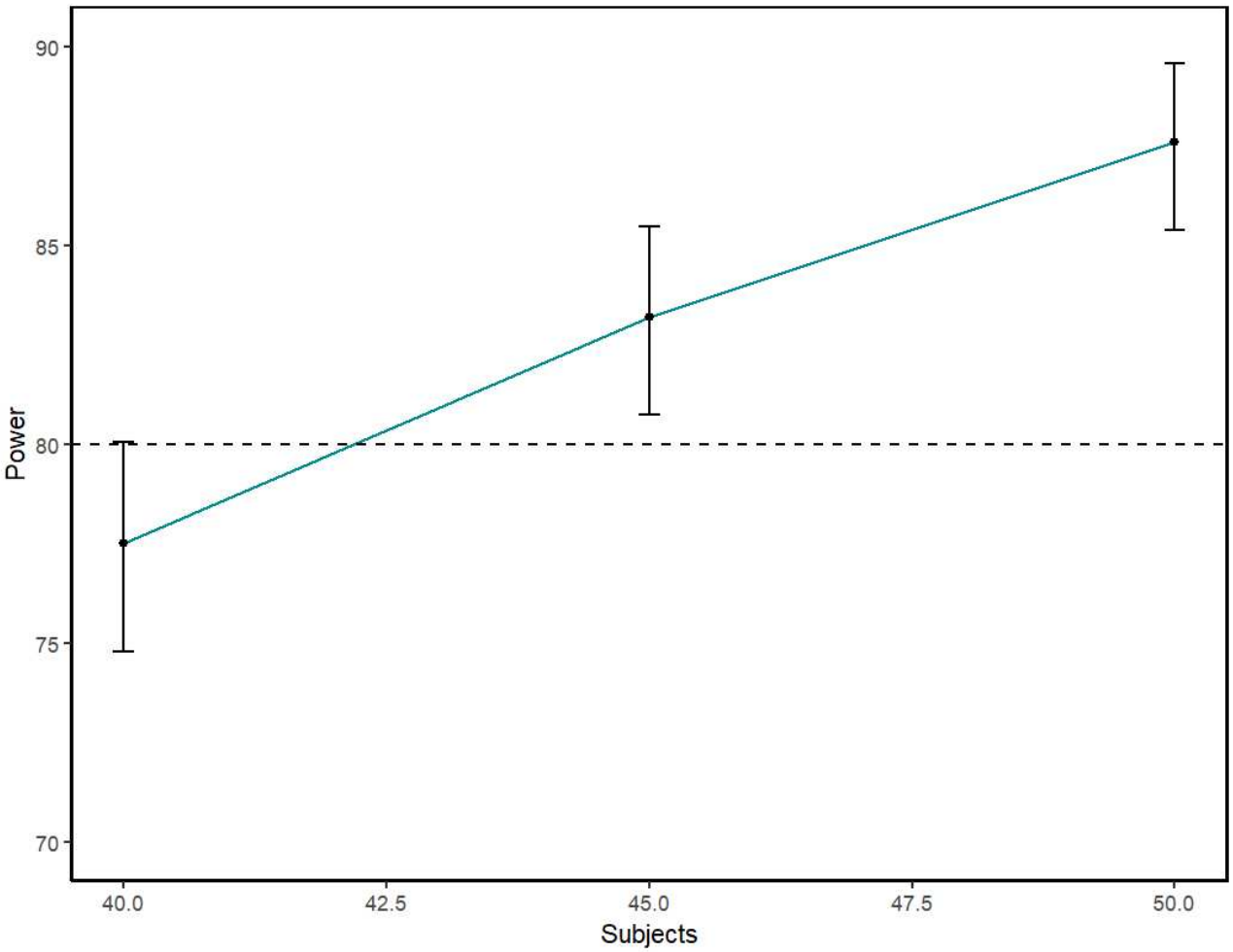

Figure 10. Power curves which shows us the power for the interaction effect between stimulus and stimulation as the sample size varies. Specifically, with sample sizes equal to 40, 45 and 50.

Discussion

The question of whether human spatial and numerical abilities are processed by the same neuro-cognitive system has been widely debated (Hayashi et al., 2013; Skagerlund et al., 2016; Walsh, 2003). In this study, we explored this hypothesis in humans by examining (a) whether the magnitude of the Delboeuf illusion is comparable for both types of quantities in a behavioral task, and (b) whether the Delboeuf illusion's strength is similarly affected for both types of quantities under different tACS stimulation frequencies. Overall, our findings do not allow for a definitive conclusion; while there is evidence supporting a generalized magnitude system, not all of our hypotheses were confirmed. Therefore, while this study points to the possibility of a generalized magnitude system, additional research is needed to validate these observations and clarify the discrepancies we found.

Our findings indicate a significant difference in human performance between discriminating continuous quantities and numbers, with participants showing much greater accuracy in distinguishing areas than in distinguishing numbers. This result is consistent with previous research, which suggests that both humans and non-human animals have a cognitive advantage when processing spatial information compared to numerical quantities (Gazzola et al., 2018.; Hubbard et al., 2005; Leibovich & Henik, 2014; Lucon-Xiccato et al., 2015). Moreover, there is conflicting evidence in the literature about the strength of the relationship between continuous and discrete quantity processing. Some studies have found weak or non-significant correlations in performance between these tasks (Cappelletti et al., 2014; Dormal et al., 2018; Droit-Volet et al., 2008), implying that the connection between continuous and discrete quantity processing might differ depending on the individual or experimental conditions. In this context, our analysis identified two notable correlations that provide additional insight into this observed discrepancy. The first correlation reveals a positive relationship between participants' ability in discriminating continuous quantities and their ability to distinguish between numerosities, aligning with prior research findings (Burr & Ross, 2008; Gebuis & Reynvoet, 2012). The second correlation shows a relationship between participants' susceptibility to the Delboeuf illusion with continuous quantities and their susceptibility to the same illusion with numerosity arrays, highlighting the impact of perceptual biases on numerical judgments (Anobile et al., 2018; Dormal et al., 2018).

Interestingly, although participants clearly perceived the standard Delboeuf illusion, our initial statistical analyses did not show a similar effect with numerical stimuli, potentially challenging the idea of a single perceptual mechanism underlying both types of quantities. However, upon further examination, the significant correlation we just mentioned emerged, suggesting a common perceptual basis after all.

It is important to note the possibility that numerical discrimination might have been more challenging for participants than continuous quantity discrimination. In the previous research, Santacà & Granziol (2023) demonstrated that humans do perceive the numerical Delboeuf illusion, which contrasts with our initial findings. This difference could be due to variations in task procedures, stimulus presentation, or the characteristics of participants between the two studies. Compared to the previous study, which was conducted online with varying devices and resolutions, the current research was performed in a controlled laboratory setting, ensuring consistent conditions such as monitor distance and the absolute size of the stimuli. Additionally, in this study, participants were exposed to stimuli for a shorter duration of 150 milliseconds per trial to prevent eye movement, unlike the 1500 milliseconds used in the previous research (Santacà & Granziol, 2023). Furthermore, the number of trials and the overall duration of the experiments varied significantly between the two studies. The earlier study lasted about 15 minutes with a total of 120 trials, including 24 illusory trials (Santacà & Granziol, 2023), whereas our study included 600 trials in total, with 60 trials involving the numerical Delboeuf illusion and 60 featuring the classic illusion. The differences in experimental setup and protocol could have influenced participants' levels of fatigue, attention, and overall performance, which should be carefully considered when interpreting and comparing the results of the two studies. Therefore, future research should carefully account for task design and methodological factors to better understand the elements that lead to variations in perceptual judgments across different quantity discrimination tasks.

In addition to assessing whether the Delboeuf illusion affects spatial and numerical quantities similarly in a behavioral task, we also examined the effect of different tACS frequencies on the illusion's strength. We found no significant interaction between tACS and the type of discrimination task, which further supports the hypothesis of a shared perceptual mechanism underlying magnitude processing. Indeed, despite observing significant effects of both stimulation and discrimination type independently, the absence of an interaction

indicates that tACS modulation of illusion strength does not significantly differ between classic and numerical discrimination tasks. An intriguing finding emerged when examining the impact of different tACS frequencies on magnitude processing. We hypothesized that theta-frequency tACS (7 Hz) over the right parietal cortex would enhance visual integration, thereby amplifying the illusion, while beta-frequency tACS (18 Hz) would weaken the illusion by promoting visual segregation. Participants underwent three tACS sessions (7 Hz, 18 Hz, and no stimulation), performing quantity discrimination tasks involving both classic and numerical Delboeuf illusions. Contrary to our hypothesis, tACS at 7 Hz targeting the parietal areas actually seemed to reduce the strength of the perceptual illusion compared to stimulation at 18 Hz. Our hypothesis was based on previous research by Stonkus et al. (2016), which showed that theta-frequency tACS applied to parietal regions can enhance perceptual integration processes. In their study, the authors found that theta tACS improved performance in tasks where participants had to identify a target stimulus (a snake composed of Gabor patches with similar orientations) among distractors (Gabor patches with different orientations). We interpreted these results as suggesting that theta tACS could enhance the spatial integration needed to resolve the Delboeuf illusion, where the perception of two identical-sized stimuli changes depending on the size of the surrounding context elements. Contrary to our expectations, our study found that theta tACS at 7 Hz weakened the strength of the illusion compared to the 18 Hz stimulation condition. The exact mechanism behind this unexpected result is not fully understood. One possible explanation is that 18 Hz tACS enhances visual segregation only when distractors are perceived as such, but in this study, the context might have been viewed as neutral by participants. On the other hand, 7 Hz tACS may enhance mechanisms that inhibit irrelevant information, such as distractors, rather than boosting perceptual integration processes. This speculation might also account for the findings of Stonkus et al. (2016), where participants needed to both integrate target stimuli and filter out distractors. In our experimental setup, although the background context was not directly related to the main task, it might have been perceived as a distractor that needed to be inhibited. However, these explanations remain speculative at this point. Interestingly, applying theta tACS to the parietal cortex was also linked to a decline in performance on visual memory tasks. This suggests that 7 Hz parietal tACS might affect not only perceptual mechanisms but also working memory processes, potentially interfering with the accurate encoding of information into working memory (Wolinski et al., 2018).

In conclusion, our study provides insights into the perceptual mechanisms behind the Delboeuf illusion by combining findings from behavioral tasks and transcranial alternating current stimulation. We found differences in performance between spatial and numerical quantity discrimination, with participants showing better ability in continuous quantity discrimination. Importantly, the lack of a significant interaction between tACS and discrimination type supports the idea of a common perceptual mechanism underlying the perception of the Delboeuf illusion, even when different magnitudes are involved. However, the numerical discrimination task was more challenging compared to a previous study (Santacà & Granziol, 2023), highlighting the need for further research to explore the factors contributing to this discrepancy. In this context, we plan to use the power analysis mentioned earlier to replicate this study with an appropriate sample size (i.e., ensuring at least 80% power). Future research could further investigate the cognitive and perceptual processes involved in numerical discrimination tasks, possibly incorporating task modifications to improve performance, such as extending the duration of stimuli presentation and using an eye tracker to account for eye movements. Moreover, studies examining the neural correlates of numerical perception could offer valuable insights into the mechanisms behind the difficulties in numerical discrimination observed in our study. These efforts will help deepen our understanding of the complexities of numerical perception and its interaction with perceptual illusions. Future research exploring the effects of tACS on other perceptual illusions could offer valuable insights into how our findings apply to different perceptual contexts. Overall, our work enhances the understanding of the perceptual processes underlying the Delboeuf illusion and highlights the potential of non-invasive brain stimulation techniques for modulating visual perception.

Bibliography

Ahn, S., Mellin, J. M., Alagapan, S., Alexander, M. L., Gilmore, J. H., Jarskog, L. F., & Fröhlich, F. (2019). Targeting reduced neural oscillations in patients with schizophrenia by transcranial alternating current stimulation. *NeuroImage*, *186*, 126–136. https://doi.org/10.1016/j.neuroimage.2018.10.056

Alekseichuk, I., Wischnewski, M., & Opitz, A. (2022). A minimum effective dose for (transcranial) alternating current stimulation. *Brain Stimulation*, *15*(5), 1221–1222. https://doi.org/10.1016/j.brs.2022.08.018

Anastassiou, C. A., Perin, R., Markram, H., & Koch, C. (2011). Ephaptic coupling of cortical neurons. *Nature Neuroscience*, *14*(2), 217–223. https://doi.org/10.1038/nn.2727

Anobile, G., Burr, D. C., Iaia, M., Marinelli, C. V., Angelelli, P., & Turi, M. (2018). Independent adaptation mechanisms for numerosity and size perception provide evidence against a common sense of magnitude. *Scientific Reports*, *8*(1), 13571. https://doi.org/10.1038/s41598-018-31893-6

Antal, A., Alekseichuk, I., Bikson, M., Brockmöller, J., Brunoni, A. R., Chen, R., Cohen, L. G., Dowthwaite, G., Ellrich, J., Flöel, A., Fregni, F., George, M. S., Hamilton, R., Haueisen, J., Herrmann, C. S., Hummel, F. C., Lefaucheur, J. P., Liebetanz, D., Loo, C. K., … Paulus, W. (2017). Low intensity transcranial electric stimulation: Safety, ethical, legal regulatory and application guidelines. *Clinical Neurophysiology*, *128*(9), 1774–1809. https://doi.org/10.1016/j.clinph.2017.06.001

Antal, A., Nitsche, M. A., Kruse, W., Kincses, T. Z., Hoffmann, K.-P., & Paulus, W. (2004). Direct Current Stimulation over V5 Enhances Visuomotor Coordination by Improving Motion Perception in Humans. *Journal of Cognitive Neuroscience*, *16*(4), 521–527. https://doi.org/10.1162/089892904323057263

Avery, G. C., & Day, R. H. (1969). Basis of the horizontal-vertical illusion. *Journal of Experimental Psychology*, *81*(2), 376–380. https://doi.org/10.1037/h0027737

Bach, M., & Meigen, T. (1997). Similar Electrophysiological Correlates of Texture Segregation Induced by Luminance, Orientation, Motion and Stereo. *Vision Research*, *37*(11), 1409–1414. https://doi.org/10.1016/S0042-6989(96)00322-7

Banton, T., & Levi, D. M. (n.d.). *Spatial Localization of Motion-Defined Luminance-Defined Contours*.

Battaglini, L., Ghiani, A., Casco, C., & Ronconi, L. (2020). Parietal tACS at beta frequency improves vision in a crowding regime. *NeuroImage*, *208*, 116451. https://doi.org/10.1016/j.neuroimage.2019.116451

Benjamini, Y., & Hochberg, Y. (1995). Controlling the False Discovery Rate: A Practical and Powerful Approach to Multiple Testing. *Journal of the Royal Statistical Society Series B: Statistical Methodology*, *57*(1), 289–300. https://doi.org/10.1111/j.2517-6161.1995.tb02031.x

Benussi, A., Cantoni, V., Grassi, M., Brechet, L., Michel, C. M., Datta, A., Thomas, C., Gazzina, S., Cotelli, M. S., Bianchi, M., Premi, E., Gadola, Y., Cotelli, M., Pengo, M., Perrone, F., Scolaro, M., Archetti, S., Solje, E., Padovani, A., … Borroni, B. (2022). Increasing Brain Gamma Activity Improves Episodic Memory and Restores Cholinergic Dysfunction in Alzheimer's Disease. *Annals of Neurology*, *92*(2), 322–334. https://doi.org/10.1002/ana.26411

Benwell, C. S. Y., Learmonth, G., Miniussi, C., Harvey, M., & Thut, G. (2015). Non-linear effects of transcranial direct current stimulation as a function of individual baseline performance: Evidence from biparietal tDCS influence on lateralized attention bias. *Cortex*, *69*, 152–165. https://doi.org/10.1016/j.cortex.2015.05.007

Bestmann, S., & Walsh, V. (2017). Transcranial electrical stimulation. *Current Biology*, *27*(23), R1258–R1262. https://doi.org/10.1016/j.cub.2017.11.001

Bex, P. J., & Dakin, S. C. (2005). Spatial interference among moving targets. *Vision Research*, *45*(11), 1385–1398. https://doi.org/10.1016/j.visres.2004.12.001

Bindman, L. J., Lippold, C. J., & Redfearn, J. W. T. (n.d.). *THE ACTION OF BRIEF POLARIZING CURRENTS ON THE CEREBRAL CORTEX OF THE RAT (I) DURING CURRENT FLOW AND (2) IN THE PRODUCTION OF LONG-LASTING AFTER-EFFECTS*.

Bisazza, A., Agrillo, C., & Lucon-Xiccato, T. (2014). Extensive training extends numerical abilities of guppies. *Animal Cognition*, *17*(6), 1413–1419. https://doi.org/10.1007/s10071-014-0759-7

Bjoertomt, O. (2002). Spatial neglect in near and far space investigated by repetitive transcranial magnetic stimulation. *Brain*, *125*(9), 2012–2022. https://doi.org/10.1093/brain/awf211

Blais, B. S., Frenkel, M. Y., Kuindersma, S. R., Muhammad, R., Shouval, H. Z., Cooper, L. N., & Bear, M. F. (2008). Recovery From Monocular Deprivation Using Binocular Deprivation. *Journal of Neurophysiology*, *100*(4), 2217–2224. https://doi.org/10.1152/jn.90411.2008

Bortoletto, M., Pellicciari, M. C., Rodella, C., & Miniussi, C. (2015). The Interaction With Task-induced Activity is More Important Than Polarization: A tDCS Study. *Brain Stimulation*, *8*(2), 269–276. https://doi.org/10.1016/j.brs.2014.11.006

Brown, S. W. (1997). Attentional resources in timing: Interference effects in concurrent temporal and nontemporal working memory tasks. *Perception & Psychophysics*, *59*(7), 1118–1140. https://doi.org/10.3758/BF03205526

Brunoni, A. R., Fregni, F., & Pagano, R. L. (2011). Translational research in transcranial direct current stimulation (tDCS): A systematic review of studies in animals. *Revneuro*, *22*(4), 471–481. https://doi.org/10.1515/rns.2011.042

Burr, D., & Ross, J. (2008). A Visual Sense of Number. *Current Biology*, *18*(6), 425–428. https://doi.org/10.1016/j.cub.2008.02.052

Butler, T. W., & Westheimer, G. (1978). Interference with stereoscopic acuity: Spatial, temporal, and disparity tuning. *Vision Research*, *18*(10), 1387–1392. https://doi.org/10.1016/0042-6989(78)90231-6

Cabral-Calderin, Y., & Wilke, M. (2020). Probing the Link Between Perception and Oscillations: Lessons from Transcranial Alternating Current Stimulation. *The Neuroscientist*, *26*(1), 57–73. https://doi.org/10.1177/1073858419828646

Calabria, M., & Rossetti, Y. (2005). Interference between number processing and line bisection: A methodology. *Neuropsychologia*, *43*(5), 779–783. https://doi.org/10.1016/j.neuropsychologia.2004.06.027

Cantlon, J. F., & Brannon, E. M. (2006). Shared System for Ordering Small and Large Numbers in Monkeys and Humans. *Psychological Science*, *17*(5), 401–406. https://doi.org/10.1111/j.1467-9280.2006.01719.x

Cantlon, J. F., Brannon, E. M., Carter, E. J., & Pelphrey, K. A. (2006). Functional Imaging of Numerical Processing in Adults and 4-y-Old Children. *PLoS Biology*, *4*(5), e125. https://doi.org/10.1371/journal.pbio.0040125

Cantlon, J. F., Libertus, M. E., Pinel, P., Dehaene, S., Brannon, E. M., & Pelphrey, K. A. (2009). The Neural Development of an Abstract Concept of Number. *Journal of Cognitive Neuroscience*, *21*(11), 2217–2229. https://doi.org/10.1162/jocn.2008.21159

Capilla, A., Arana, L., García-Huéscar, M., Melcón, M., Gross, J., & Campo, P. (2022). The natural frequencies of the resting human brain: An MEG-based atlas. *NeuroImage*, *258*, 119373. https://doi.org/10.1016/j.neuroimage.2022.119373

Cappelletti, M., Chamberlain, R., Freeman, E. D., Kanai, R., Butterworth, B., Price, C. J., & Rees, G. (2014). Commonalities for Numerical and Continuous Quantity Skills at Temporo-parietal Junction. *Journal of Cognitive Neuroscience*, *26*(5), 986–999. https://doi.org/10.1162/jocn_a_00546

Caputo, G., & Casco, C. (1999). A visual evoked potential correlate of global figure-ground segmentation. *Vision Research*, *39*(9), 1597–1610. https://doi.org/10.1016/S0042-6989(98)00270-3

Casini, L., & Macar, F. (1997). Effects of attention manipulation on judgments of duration and of intensity in the visual modality. *Memory & Cognition*, *25*(6), 812–818. https://doi.org/10.3758/BF03211325

Chicherov, V., Plomp, G., & Herzog, M. H. (2014). Neural correlates of visual crowding. *NeuroImage*, *93*, 23–31. https://doi.org/10.1016/j.neuroimage.2014.02.021

Cho, K. K., & Bear, M. F. (2009). Promoting neurological recovery of function via metaplasticity. *Future Neurology*, *5*(1), 21–26. https://doi.org/10.2217/fnl.09.62

Chung, S. T. L. (2002). *The Effect of Letter Spacing on Reading Speed in Central and Peripheral Vision*. *43*(4).

Chung, S. T. L., Levi, D. M., & Legge, G. E. (2001). Spatial-frequency and contrast properties of crowding. *Vision Research*, *41*(14), 1833–1850. https://doi.org/10.1016/S0042-6989(01)00071-2

Chung, S. T. L., Li, R. W., & Levi, D. M. (2007). Crowding between first- and second-order letter stimuli in normal foveal and peripheral vision. *Journal of Vision*, *7*(2), 10. https://doi.org/10.1167/7.2.10

Chung, S. T. L., Mansfield, J. S., & Legge, G. E. (1998). Psychophysics of reading. XVIII. The effect of print size on reading speed in normal peripheral vision. *Vision Research*, *38*(19), 2949–2962. https://doi.org/10.1016/S0042-6989(98)00072-8

Cordes, S., Gelman, R., Gallistel, C. R., & Whalen, J. (2001). Variability signatures distinguish verbal from nonverbal counting for both large and small numbers. *Psychonomic Bulletin & Review*, *8*(4), 698–707. https://doi.org/10.3758/BF03196206

De Hevia, M.-D., Girelli, L., Bricolo, E., & Vallar, G. (2008). The representational space of numerical magnitude: Illusions of length. *Quarterly Journal of Experimental Psychology*, *61*(10), 1496–1514. https://doi.org/10.1080/17470210701560674

Dehaene, S. (2009). Origins of Mathematical Intuitions: The Case of Arithmetic. *Annals of the New York Academy of Sciences*, *1156*(1), 232–259. https://doi.org/10.1111/j.1749-6632.2009.04469.x

Dehaene, S., Bossini, S., & Giraux, P. (1993). The mental representation of parity and number magnitude. *Journal of Experimental Psychology: General*, *122*(3), 371–396. https://doi.org/10.1037/0096-3445.122.3.371

Dehaene, S., & Changeux, J.-P. (1993). Development of Elementary Numerical Abilities: A Neuronal Model. *Journal of Cognitive Neuroscience*, *5*(4), 390–407. https://doi.org/10.1162/jocn.1993.5.4.390

Dehaene, S., Dehaene-Lambertz, G., & Cohen, L. (1998). Abstract representations of numbers in the animal and human brain. *Trends in Neurosciences*, *21*(8), 355–361. https://doi.org/10.1016/S0166-2236(98)01263-6

Dehaene, S., Spelke, E., Pinel, P., Stanescu, R., & Tsivkin, S. (1999). Sources of Mathematical Thinking: Behavioral and Brain-Imaging Evidence. *Science*, *284*(5416), 970–974. https://doi.org/10.1126/science.284.5416.970

Di Dona, G., Zamfira, D. A., Battista, M., Battaglini, L., Perani, D., & Ronconi, L. (2024). The role of parietal beta-band activity in the resolution of visual crowding. *NeuroImage*, *289*, 120550. https://doi.org/10.1016/j.neuroimage.2024.120550

Dormal, V., Andres, M., & Pesenti, M. (2008). Dissociation of numerosity and duration processing in the left intraparietal sulcus: A transcranial magnetic stimulation study. *Cortex*, *44*(4), 462–469. https://doi.org/10.1016/j.cortex.2007.08.011

Dormal, V., Larigaldie, N., Lefèvre, N., Pesenti, M., & Andres, M. (2018). Effect of perceived length on numerosity estimation: Evidence from the Müller-Lyer illusion. *Quarterly Journal of Experimental Psychology*, *71*(10), 2142–2151. https://doi.org/10.1177/1747021817738720

Droit-Volet, S., Clément, A., & Fayol, M. (2008). Time, Number and Length: Similarities and Differences in Discrimination in Adults and Children. *Quarterly Journal of Experimental Psychology*, *61*(12), 1827–1846. https://doi.org/10.1080/17470210701743643

Evans, I., Palmisano, S., & Croft, R. J. (2022). Effect of ambient lighting on frequency dependence in transcranial electrical stimulation-induced phosphenes. *Scientific Reports*, *12*(1), 7775. https://doi.org/10.1038/s41598-022-11755-y

Fahle, M., Quenzer, T., Braun, C., & Spang, K. (2003). Feature-specific electrophysiological correlates of texture segregation. *Vision Research*, *43*(1), 7–19. https://doi.org/10.1016/S0042-6989(02)00265-1

Feigenson, L., Carey, S., & Hauser, M. (2002). The Representations Underlying Infants' Choice of More: Object Files Versus Analog Magnitudes. *Psychological Science*, *13*(2), 150–156. https://doi.org/10.1111/1467-9280.00427

Feigenson, L., Dehaene, S., & Spelke, E. (2004). Core systems of number. *Trends in Cognitive Sciences*, *8*(7), 307–314. https://doi.org/10.1016/j.tics.2004.05.002

Fertonani, A., Ferrari, C., & Miniussi, C. (2015). What do you feel if I apply transcranial electric stimulation? Safety, sensations and secondary induced effects. *Clinical Neurophysiology*, *126*(11), 2181–2188. https://doi.org/10.1016/j.clinph.2015.03.015

Fertonani, A., Pirulli, C., & Miniussi, C. (2011). Random Noise Stimulation Improves Neuroplasticity in Perceptual Learning. *The Journal of Neuroscience*, *31*(43), 15416–15423. https://doi.org/10.1523/JNEUROSCI.2002-11.2011

Fiene, M., Schwab, B. C., Misselhorn, J., Herrmann, C. S., Schneider, T. R., & Engel, A. K. (2020). Phase-specific manipulation of rhythmic brain activity by transcranial alternating current stimulation. *Brain Stimulation*, *13*(5), 1254–1262. https://doi.org/10.1016/j.brs.2020.06.008

Finger, F. W., & Spelt, D. K. (1947). The illustration of the horizontal-vertical illusion. *Journal of Experimental Psychology*, *37*(3), 243–250. https://doi.org/10.1037/h0055605

Fischer, M. H., Castel, A. D., Dodd, M. D., & Pratt, J. (2003). Perceiving numbers causes spatial shifts of attention. *Nature Neuroscience*, *6*(6), 555–556. https://doi.org/10.1038/nn1066

Foxe, J. J., & Snyder, A. C. (2011). The Role of Alpha-Band Brain Oscillations as a Sensory Suppression Mechanism during Selective Attention. *Frontiers in Psychology*, *2*. https://doi.org/10.3389/fpsyg.2011.00154

Francis, J. T., Gluckman, B. J., & Schiff, S. J. (2003). Sensitivity of Neurons to Weak Electric Fields. *The Journal of Neuroscience*, *23*(19), 7255–7261. https://doi.org/10.1523/JNEUROSCI.23-19-07255.2003

Frank, M. C., Everett, D. L., Fedorenko, E., & Gibson, E. (2008). Number as a cognitive technology: Evidence from Pirahã language and cognition. *Cognition*, *108*(3), 819–824. https://doi.org/10.1016/j.cognition.2008.04.007

Gallistel, C. R., & Gelman, R. (2000). Non-verbal numerical cognition: From reals to integers. *Trends in Cognitive Sciences*, *4*(2), 59–65. https://doi.org/10.1016/S1364-6613(99)01424-2

Gartside, I. B. (1968). Mechanisms of Sustained Increases of Firing Rate of Neurones in the Rat Cerebral Cortex after Polarization: Role of Protein Synthesis. *Nature*, *220*(5165), 383–384. https://doi.org/10.1038/220383a0

Gazzola, A., Vallortigara, G., & Pellitteri-Rosa, D. (n.d.). *Continuous and discrete quantity discrimination in tortoises*.

Gebuis, T., & Reynvoet, B. (2012). The Role of Visual Information in Numerosity Estimation. *PLoS ONE*, *7*(5), e37426. https://doi.org/10.1371/journal.pone.0037426

Gerstmann, J. (1940). SYNDROME OF FINGER AGNOSIA, DISORIENTATION FOR RIGHT AND LEFT, AGRAPHIA AND ACALCULIA: LOCAL DIAGNOSTIC VALUE. *Archives of Neurology & Psychiatry*, *44*(2), 398. https://doi.org/10.1001/archneurpsyc.1940.02280080158009

Göbel, S., Walsh, V., & Rushworth, M. F. S. (2001). The Mental Number Line and the Human Angular Gyrus. *NeuroImage*, *14*(6), 1278–1289. https://doi.org/10.1006/nimg.2001.0927

Green, P., & MacLeod, C. J. (2016). SIMR: An R package for power analysis of generalized linear mixed models by simulation. *Methods in Ecology and Evolution*, *7*(4), 493–498. https://doi.org/10.1111/2041-210X.12504

Halberda, J., Ly, R., Wilmer, J. B., Naiman, D. Q., & Germine, L. (2012). Number sense across the lifespan as revealed by a massive Internet-based sample. *Proceedings of the National Academy of Sciences*, *109*(28), 11116–11120. https://doi.org/10.1073/pnas.1200196109

Halberda, J., Mazzocco, M. M. M., & Feigenson, L. (2008). Individual differences in non-verbal number acuity correlate with maths achievement. *Nature*, *455*(7213), 665–668. https://doi.org/10.1038/nature07246

Hariharan, S., Levi, D. M., & Klein, S. A. (2005). "Crowding" in normal and amblyopic vision assessed with Gaussian and Gabor C's. *Vision Research*, *45*(5), 617–633. https://doi.org/10.1016/j.visres.2004.09.035

Harris, J. K. (2021). Primer on binary logistic regression. *Family Medicine and Community Health*, *9*(Suppl 1), e001290. https://doi.org/10.1136/fmch-2021-001290

Hayashi, M. J., Kanai, R., Tanabe, H. C., Yoshida, Y., Carlson, S., Walsh, V., & Sadato, N. (2013). Interaction of Numerosity and Time in Prefrontal and Parietal Cortex. *The Journal of Neuroscience*, *33*(3), 883–893. https://doi.org/10.1523/JNEUROSCI.6257-11.2013

Helfrich, R. F., Schneider, T. R., Rach, S., Trautmann-Lengsfeld, S. A., Engel, A. K., & Herrmann, C. S. (2014). Entrainment of Brain Oscillations by Transcranial Alternating Current Stimulation. *Current Biology*, *24*(3), 333–339. https://doi.org/10.1016/j.cub.2013.12.041

Higashiyama, A. (1992). Anisotropic perception of visual angle: Implications for the horizontal-vertical illusion, overconstancy of size, and the moon illusion. *Perception & Psychophysics*, *51*(3), 218–230. https://doi.org/10.3758/BF03212248

Huang, W. A., Stitt, I. M., Negahbani, E., Passey, D. J., Ahn, S., Davey, M., Dannhauer, M., Doan, T. T., Hoover, A. C., Peterchev, A. V., Radtke-Schuller, S., & Fröhlich, F. (2021). Transcranial alternating current stimulation entrains alpha oscillations by preferential phase synchronization of fast-spiking cortical neurons to stimulation waveform. *Nature Communications*, *12*(1), 3151. https://doi.org/10.1038/s41467-021-23021-2

Huang, Y., Liu, A. A., Lafon, B., Friedman, D., Dayan, M., Wang, X., Bikson, M., Doyle, W. K., Devinsky, O., & Parra, L. C. (2017). Measurements and models of electric fields in the in vivo human brain during transcranial electric stimulation. *eLife*, *6*, e18834. https://doi.org/10.7554/eLife.18834

Hubbard, E. M., Piazza, M., Pinel, P., & Dehaene, S. (2005). Interactions between number and space in parietal cortex. *Nature Reviews Neuroscience*, *6*(6), 435–448. https://doi.org/10.1038/nrn1684

Hyde, D. C., Boas, D. A., Blair, C., & Carey, S. (2010). Near-infrared spectroscopy shows right parietal specialization for number in pre-verbal infants. *NeuroImage*, *53*(2), 647–652. https://doi.org/10.1016/j.neuroimage.2010.06.030

Izard, V., Sann, C., Spelke, E. S., & Streri, A. (2009). Newborn infants perceive abstract numbers. *Proceedings of the National Academy of Sciences*, *106*(25), 10382–10385. https://doi.org/10.1073/pnas.0812142106

Jacobson, L., Koslowsky, M., & Lavidor, M. (2012). tDCS polarity effects in motor and cognitive domains: A meta-analytical review. *Experimental Brain Research*, *216*(1), 1–10. https://doi.org/10.1007/s00221-011-2891-9

Jefferys, J. G. R., Deans, J., Bikson, M., & Fox, J. (2003). Effects of weak electric fields on the activity of neurons and neuronal networks. *Radiation Protection Dosimetry*, *106*(4), 321–323. https://doi.org/10.1093/oxfordjournals.rpd.a006367

Kasten, F. H., Dowsett, J., & Herrmann, C. S. (2016). Sustained Aftereffect of α-tACS Lasts Up to 70 min after Stimulation. *Frontiers in Human Neuroscience*, *10*. https://doi.org/10.3389/fnhum.2016.00245

Kasten, F. H., & Herrmann, C. S. (2019). Recovering Brain Dynamics During Concurrent tACS-M/EEG: An Overview of Analysis Approaches and Their Methodological and Interpretational Pitfalls. *Brain Topography*, *32*(6), 1013–1019. https://doi.org/10.1007/s10548-019-00727-7

Kaufmann, L., Koppelstaetter, F., Delazer, M., Siedentopf, C., Rhomberg, P., Golaszewski, S., Felber, S., & Ischebeck, A. (2005). Neural correlates of distance and congruity effects in a numerical Stroop task: An event-related fMRI study. *NeuroImage*, *25*(3), 888–898. https://doi.org/10.1016/j.neuroimage.2004.12.041

Kitajo, K., Nozaki, D., Ward, L. M., & Yamamoto, Y. (2003). Behavioral Stochastic Resonance within the Human Brain. *Physical Review Letters*, *90*(21), 218103. https://doi.org/10.1103/PhysRevLett.90.218103

Krause, M. R., Vieira, P. G., Thivierge, J.-P., & Pack, C. C. (2022). Brain stimulation competes with ongoing oscillations for control of spike timing in the primate brain. *PLOS Biology*, *20*(5), e3001650. https://doi.org/10.1371/journal.pbio.3001650

Leibovich, T., & Henik, A. (2014). Comparing Performance in Discrete and Continuous Comparison Tasks. *Quarterly Journal of Experimental Psychology*, *67*(5), 899–917. https://doi.org/10.1080/17470218.2013.837940

Lenzi, M., Furlong, M. J., Dowdy, E., Sharkey, J., Gini, G., & Altoè, G. (2015). The quantity and variety across domains of psychological and social assets associated with school victimization. *Psychology of Violence*, *5*(4), 411–421. https://doi.org/10.1037/a0039696

Levi, D. M. (2008). Crowding—An essential bottleneck for object recognition: A mini-review. *Vision Research*, *48*(5), 635–654. https://doi.org/10.1016/j.visres.2007.12.009

Levi, D. M., Hariharan, S., & Klein, S. A. (2002). Suppressive and facilitatory spatial interactions in peripheral vision: Peripheral crowding is neither size invariant nor simple contrast masking. *Journal of Vision*, *2*(2), 3–3. https://doi.org/10.1167/2.2.3

Levi, D. M., Klein, S. A., & Aitsebaomo, A. P. (1985). Vernier acuity, crowding and cortical magnification. *Vision Research*, *25*(7), 963–977. https://doi.org/10.1016/0042-6989(85)90207-X

Levi, D. M., Klein, S. A., & Hariharan, S. (2002). Suppressive and facilitatory spatial interactions in foveal vision: Foveal crowding is simple contrast masking. *Journal of Vision*, *2*(2), 2–2. https://doi.org/10.1167/2.2.2

Levi, D. M., Song, S., & Pelli, D. G. (2007). Amblyopic reading is crowded. *Journal of Vision*, *7*(2), 21. https://doi.org/10.1167/7.2.21

Levi, D. M., Toet, A., Tripathy, S. P., & Kooi, F. L. (1994). The effect of similarity and duration on spatial interaction in peripheral vision. *Spatial Vision*, *8*(2), 255–279. https://doi.org/10.1163/156856894X00350

Liebetanz, D. (2002). Pharmacological approach to the mechanisms of transcranial DC-stimulation-induced after-effects of human motor cortex excitability. *Brain*, *125*(10), 2238–2247. https://doi.org/10.1093/brain/awf238

Liu, A., Vöröslakos, M., Kronberg, G., Henin, S., Krause, M. R., Huang, Y., Opitz, A., Mehta, A., Pack, C. C., Krekelberg, B., Berényi, A., Parra, L. C., Melloni, L., Devinsky, O., & Buzsáki, G. (2018). Immediate neurophysiological effects of transcranial electrical stimulation. *Nature Communications*, *9*(1), 5092. https://doi.org/10.1038/s41467-018-07233-7

Liu, L., & Arditi, A. (2000). Apparent string shortening concomitant with letter crowding. *Vision Research*, *40*(9), 1059–1067. https://doi.org/10.1016/S0042-6989(99)00247-3

Liu, T., Jiang, Y., Sun, X., & He, S. (2009). Reduction of the Crowding Effect in Spatially Adjacent but Cortically Remote Visual Stimuli. *Current Biology*, *19*(2), 127–132. https://doi.org/10.1016/j.cub.2008.11.065

Livne, T., & Sagi, D. (2007). Configuration influence on crowding. *Journal of Vision*, *7*(2), 4. https://doi.org/10.1167/7.2.4

Louie, E. G., Bressler, D. W., & Whitney, D. (2007). Holistic crowding: Selective interference between configural representations of faces in crowded scenes. *Journal of Vision*, *7*(2), 24. https://doi.org/10.1167/7.2.24

Lucon-Xiccato, T., Miletto Petrazzini, M. E., Agrillo, C., & Bisazza, A. (2015). Guppies discriminate between two quantities of food items but prioritize item size over total amount. *Animal Behaviour*, *107*, 183–191. https://doi.org/10.1016/j.anbehav.2015.06.019

Machilsen, B., & Wagemans, J. (2011). Integration of contour and surface information in shape detection. *Vision Research*, *51*(1), 179–186. https://doi.org/10.1016/j.visres.2010.11.005

Mamassian, P., & De Montalembert, M. (2010). A simple model of the vertical–horizontal illusion. *Vision Research*, *50*(10), 956–962. https://doi.org/10.1016/j.visres.2010.03.005

Mathes, B., Trenner, D., & Fahle, M. (2006). The electrophysiological correlate of contour integration is modulated by task demands. *Brain Research*, *1114*(1), 98–112. https://doi.org/10.1016/j.brainres.2006.07.068

Miletto Petrazzini, M. E., & Brennan, C. H. (2020). Application of an abstract concept across magnitude dimensions by fish. *Scientific Reports*, *10*(1), 16935. https://doi.org/10.1038/s41598-020-74037-5

Miniussi, C., Harris, J. A., & Ruzzoli, M. (2013). Modelling non-invasive brain stimulation in cognitive neuroscience. *Neuroscience & Biobehavioral Reviews*, *37*(8), 1702–1712. https://doi.org/10.1016/j.neubiorev.2013.06.014

Motter, B. C. (2006). Modulation of Transient and Sustained Response Components of V4 Neurons by Temporal Crowding in Flashed Stimulus Sequences. *The Journal of Neuroscience*, *26*(38), 9683–9694. https://doi.org/10.1523/JNEUROSCI.5495-05.2006

Murray, M. M., Wylie, G. R., Higgins, B. A., Javitt, D. C., Schroeder, C. E., & Foxe, J. J. (2002). The Spatiotemporal Dynamics of Illusory Contour Processing: Combined High-Density Electrical Mapping, Source Analysis, and Functional Magnetic Resonance Imaging. *The Journal of Neuroscience*, *22*(12), 5055–5073. https://doi.org/10.1523/JNEUROSCI.22-12-05055.2002

Neri, P., & Levi, D. M. (2006). Spatial Resolution for Feature Binding Is Impaired in Peripheral and Amblyopic Vision. *Journal of Neurophysiology*, *96*(1), 142–153. https://doi.org/10.1152/jn.01261.2005

Nieder, A., & Dehaene, S. (2009). Representation of Number in the Brain. *Annual Review of Neuroscience*, *32*(1), 185–208. https://doi.org/10.1146/annurev.neuro.051508.135550

Nieder, A., & Miller, E. K. (2004). A parieto-frontal network for visual numerical information in the monkey. *Proceedings of the National Academy of Sciences*, *101*(19), 7457–7462. https://doi.org/10.1073/pnas.0402239101

Nitsche, M. A., & Paulus, W. (2000). Excitability changes induced in the human motor cortex by weak transcranial direct current stimulation. *The Journal of Physiology*, *527*(3), 633–639. https://doi.org/10.1111/j.1469-7793.2000.t01-1-00633.x

Odic, D., & Starr, A. (2018). An Introduction to the Approximate Number System. *Child Development Perspectives*, *12*(4), 223–229. https://doi.org/10.1111/cdep.12288

Onoe, H., Komori, M., Onoe, K., Takechi, H., Tsukada, H., & Watanabe, Y. (2001). Cortical Networks Recruited for Time Perception: A Monkey Positron Emission Tomography (PET) Study. *NeuroImage*, *13*(1), 37–45. https://doi.org/10.1006/nimg.2000.0670

Opitz, A., Falchier, A., Yan, C.-G., Yeagle, E. M., Linn, G. S., Megevand, P., Thielscher, A., Deborah A., R., Milham, M. P., Mehta, A. D., & Schroeder, C. E. (2016). Spatiotemporal structure of intracranial electric fields induced by transcranial electric stimulation in humans and nonhuman primates. *Scientific Reports*, *6*(1), 31236. https://doi.org/10.1038/srep31236

Parkes, L., Lund, J., Angelucci, A., Solomon, J. A., & Morgan, M. (2001). Compulsory averaging of crowded orientation signals in human vision. *Nature Neuroscience*, *4*(7), 739–744. https://doi.org/10.1038/89532

Paulus, W. (2011). Transcranial electrical stimulation (tES – tDCS; tRNS, tACS) methods. *Neuropsychological Rehabilitation*, *21*(5), 602–617. https://doi.org/10.1080/09602011.2011.557292

Pecunioso, A., Miletto Petrazzini, M. E., & Agrillo, C. (2020). Anisotropy of perceived numerosity: Evidence for a horizontal–vertical numerosity illusion. *Acta Psychologica*, *205*, 103053. https://doi.org/10.1016/j.actpsy.2020.103053

Pei, F., Pettet, M. W., Vildavski, V. Y., & Norcia, A. M. (n.d.). *Event-related potentials show con¢gural speci¢city of global form processing*.

Pelli, D. G. (2008). Crowding: A cortical constraint on object recognition. *Current Opinion in Neurobiology*, *18*(4), 445–451. https://doi.org/10.1016/j.conb.2008.09.008

Pelli, D. G., Palomares, M., & Majaj, N. J. (2004). Crowding is unlike ordinary masking: Distinguishing feature integration from detection. *Journal of Vision*, *4*(12), 12. https://doi.org/10.1167/4.12.12

Pelli, D. G., Tillman, K. A., Freeman, J., Su, M., Berger, T. D., & Majaj, N. J. (2007). Crowding and eccentricity determine reading rate. *Journal of Vision*, *7*(2), 20. https://doi.org/10.1167/7.2.20

Piazza, M., & Eger, E. (2016). Neural foundations and functional specificity of number representations. *Neuropsychologia*, *83*, 257–273. https://doi.org/10.1016/j.neuropsychologia.2015.09.025

Piazza, M., Mechelli, A., Price, C. J., & Butterworth, B. (2006). Exact and approximate judgements of visual and auditory numerosity: An fMRI study. *Brain Research*, *1106*(1), 177–188. https://doi.org/10.1016/j.brainres.2006.05.104

Picon, E., Dramkin, D., & Odic, D. (2019). Visual illusions help reveal the primitives of number perception. *Journal of Experimental Psychology: General*, *148*(10), 1675–1687. https://doi.org/10.1037/xge0000553

Rao, S. M., Mayer, A. R., & Harrington, D. L. (2001). The evolution of brain activation during temporal processing. *Nature Neuroscience*, *4*(3), 317–323. https://doi.org/10.1038/85191

Robertson, L. C. (2003). Binding, spatial attention and perceptual awareness. *Nature Reviews Neuroscience*, *4*(2), 93–102. https://doi.org/10.1038/nrn1030

Roelfsema, P. R. (2006). *CORTICAL ALGORITHMS FOR PERCEPTUAL GROUPING*.

Roitman, J. D., & Brannon, E. M. (2003). *Nonverbal Representations of Time and Number in Animals and Human Infants*.

Ronconi, L., & Bellacosa Marotti, R. (2017). Awareness in the crowd: Beta power and alpha phase of prestimulus oscillations predict object discrimination in visual crowding. *Consciousness and Cognition*, *54*, 36–46. https://doi.org/10.1016/j.concog.2017.04.020

Ronconi, L., Bertoni, S., & Bellacosa Marotti, R. (2016). The neural origins of visual crowding as revealed by event-related potentials and oscillatory dynamics. *Cortex*, *79*, 87–98. https://doi.org/10.1016/j.cortex.2016.03.005

Samaha, J., Gosseries, O., & Postle, B. R. (2017). Distinct Oscillatory Frequencies Underlie Excitability of Human Occipital and Parietal Cortex. *The Journal of Neuroscience*, *37*(11), 2824–2833. https://doi.org/10.1523/JNEUROSCI.3413-16.2017

San-Juan, D., Espinoza-López, D. A., Vázquez-Gregorio, R., Trenado, C., Aragón, M. F.-G., Pérez-Pérez, D., Hernández-Ruiz, A., & Anschel, D. J. (2022). A pilot randomized controlled clinical trial of Transcranial Alternating Current Stimulation in patients with multifocal pharmaco-resistant epilepsy. *Epilepsy & Behavior*, *130*, 108676. https://doi.org/10.1016/j.yebeh.2022.108676

Santacà, M., & Granziol, U. (2023). The influence of visual illusion perception on numerosity estimation could be evolutionarily conserved: Exploring the numerical Delboeuf illusion in humans (Homo sapiens) and fish (Poecilia reticulata). *Animal Cognition*, *26*(3), 823–835. https://doi.org/10.1007/s10071-022-01721-6

Sawamura, H., Shima, K., & Tanji, J. (2002). Numerical representation for action in the parietal cortex of the monkey. *Nature*, *415*(6874), 918–922. https://doi.org/10.1038/415918a

Shpaner, M., Molholm, S., Forde, E., & Foxe, J. J. (2013). Disambiguating the roles of area V1 and the lateral occipital complex (LOC) in contour integration. *NeuroImage*, *69*, 146–156. https://doi.org/10.1016/j.neuroimage.2012.11.023

Siegler, R. S., & Opfer, J. E. (2003). The Development of Numerical Estimation: Evidence for Multiple Representations of Numerical Quantity. *Psychological Science*, *14*(3), 237–250. https://doi.org/10.1111/1467-9280.02438

Simon, O., Mangin, J.-F., Cohen, L., Le Bihan, D., & Dehaene, S. (2002). Topographical Layout of Hand, Eye, Calculation, and Language-Related Areas in the Human Parietal Lobe. *Neuron*, *33*(3), 475–487. https://doi.org/10.1016/S0896-6273(02)00575-5

Skagerlund, K., Karlsson, T., & Träff, U. (2016). Magnitude Processing in the Brain: An fMRI Study of Time, Space, and Numerosity as a Shared Cortical System. *Frontiers in Human Neuroscience*, *10*. https://doi.org/10.3389/fnhum.2016.00500

Starr, A., Libertus, M. E., & Brannon, E. M. (2013). Number sense in infancy predicts mathematical abilities in childhood. *Proceedings of the National Academy of Sciences*, *110*(45), 18116–18120. https://doi.org/10.1073/pnas.1302751110

Stonkus, R., Braun, V., Kerlin, J. R., Volberg, G., & Hanslmayr, S. (2016). Probing the causal role of prestimulus interregional synchrony for perceptual integration via tACS. *Scientific Reports*, *6*(1), 32065. https://doi.org/10.1038/srep32065

Strasburger, H., Harvey, L. O., & Rentschler, I. (1991). Contrast thresholds for identification of numeric characters in direct and eccentric view. *Perception & Psychophysics*, *49*(6), 495–508. https://doi.org/10.3758/BF03212183

Toet, A., & Levi, D. M. (1992). The two-dimensional shape of spatial interaction zones in the parafovea. *Vision Research*, *32*(7), 1349–1357. https://doi.org/10.1016/0042-6989(92)90227-A

Tootell, R. B. H., Hadjikhani, N., Hall, E. K., Marrett, S., Vanduffel, W., Vaughan, J. T., & Dale, A. M. (1998). The Retinotopy of Visual Spatial Attention. *Neuron*, *21*(6), 1409–1422. https://doi.org/10.1016/S0896-6273(00)80659-5

Van Marle, K., Chu, F. W., Li, Y., & Geary, D. C. (2014). Acuity of the approximate number system and preschoolers' quantitative development. *Developmental Science*, *17*(4), 492–505. https://doi.org/10.1111/desc.12143

Vöröslakos, M., Takeuchi, Y., Brinyiczki, K., Zombori, T., Oliva, A., Fernández-Ruiz, A., Kozák, G., Kincses, Z. T., Iványi, B., Buzsáki, G., & Berényi, A. (2018). Direct effects of transcranial electric stimulation on brain circuits in rats and humans. *Nature Communications*, *9*(1), 483. https://doi.org/10.1038/s41467-018-02928-3

Vos, P. G., Van Oeffelen, M. P., Tibosch, H. J., & Allik, J. (1988). Interactions between area and numerosity. *Psychological Research*, *50*(3), 148–154. https://doi.org/10.1007/BF00310175

Walsh, V. (2003). A theory of magnitude: Common cortical metrics of time, space and quantity. *Trends in Cognitive Sciences*, *7*(11), 483–488. https://doi.org/10.1016/j.tics.2003.09.002

Westheimer, G., Shimamura, K., & McKee, S. P. (1976). Interference with line-orientation sensitivity*. *Journal of the Optical Society of America*, *66*(4), 332. https://doi.org/10.1364/JOSA.66.000332

Wilson, F. A. W., Scalaidhe, S. P. Ó., & Goldman-Rakic, P. S. (1993). Dissociation of Object and Spatial Processing Domains in Primate Prefrontal Cortex. *Science*, *260*(5116), 1955–1958. https://doi.org/10.1126/science.8316836

Wischnewski, M., Alekseichuk, I., & Opitz, A. (2023). Neurocognitive, physiological, and biophysical effects of transcranial alternating current stimulation. *Trends in Cognitive Sciences*, *27*(2), 189–205. https://doi.org/10.1016/j.tics.2022.11.013

Wischnewski, M., Engelhardt, M., Salehinejad, M. A., Schutter, D. J. L. G., Kuo, M.-F., & Nitsche, M. A. (2019). NMDA Receptor-Mediated Motor Cortex Plasticity After 20 Hz Transcranial Alternating Current Stimulation. *Cerebral Cortex*, *29*(7), 2924–2931. https://doi.org/10.1093/cercor/bhy160

Wischnewski, M., & Schutter, D. J. L. G. (2017). After-effects of transcranial alternating current stimulation on evoked delta and theta power. *Clinical Neurophysiology*, *128*(11), 2227–2232. https://doi.org/10.1016/j.clinph.2017.08.029

Wischnewski, M., Zerr, P., & Schutter, D. J. L. G. (2016). Effects of Theta Transcranial Alternating Current Stimulation Over the Frontal Cortex on Reversal Learning. *Brain Stimulation*, *9*(5), 705–711. https://doi.org/10.1016/j.brs.2016.04.011

Wolinski, N., Cooper, N. R., Sauseng, P., & Romei, V. (2018). The speed of parietal theta frequency drives visuospatial working memory capacity. *PLOS Biology*, *16*(3), e2005348. https://doi.org/10.1371/journal.pbio.2005348

Yavari, F., Jamil, A., Mosayebi Samani, M., Vidor, L. P., & Nitsche, M. A. (2018). Basic and functional effects of transcranial Electrical Stimulation (tES)—An introduction. *Neuroscience & Biobehavioral Reviews*, *85*, 81–92. https://doi.org/10.1016/j.neubiorev.2017.06.015

Zorzi, M., Priftis, K., & Umiltà, C. (2002). Neglect disrupts the mental number line. *Nature*, *417*(6885), 138–139. https://doi.org/10.1038/417138a

Supplementary Material

Table S1. Humans' individual performance (small, large, congruent, incongruent trials: frequency of choices for the larger numerosity and area; Delboeuf illusion: frequency of choices for the expected larger numerosity, i.e., presented in the small background). Statistics were calculated with binomial tests for individual analyses. Asterisks (*) denote a significant departure from chance level (0.5). This statistics allows us to understand whether each subject's performance in each experimental condition is different from chance level. Particularly in control trials they indicate whether they can discriminate the largest/more numerous stimulus. In the illusory ones whether they perceive the classical/numerical Delboeuf illusion.

			Continuous quantity discrimination					Numerical discrimination					
Subject	**Age**	**Gender**	**Small**	**Large**	**Congruent**	**Incongruent**	**Delboeuf illusion**	**Small**	**Large**	**Congruent**	**Incongruent**	**Delboeuf illusion**	**tAcs**
1	**24**	**F**	**50/60**	**56/60**	**1/59**	**60/60**	**60/60**	**54/59**	**53/60**	**49/60**	**58/60**	**40/60**	**Sham**
			p<0.001*	**p<0.001***	**p<0.001***	**p<0.001***	**p<0.001***	**p<0.001***	**p<0.001***	**p<0.001***	**p<0.001***	**p=0.013***	
			51/59	**55/60**	**1/59**	**60/60**	**60/60**	**46/56**	**51/60**	**46/58**	**53/60**	**43/60**	**7 Hz**
			p<0.001*	**p<0.001***	**p<0.001***	**p<0.001***	**p<0.001***	**p<0.001***	**p<0.001***	**p<0.001***	**p<0.001***	**p=0.001***	
			48/60	**48/57**	**4/60**	**60/60**	**60/60**	**46/59**	**48/57**	**45/60**	**51/58**	**30/59**	**18 Hz**
			p<0.001*	**p<0.001***	**p<0.001***	**p<0.001***	**p<0.001***	**p<0.001***	**p<0.001***	**p<0.001***	**p<0.001***	**p=1.000**	
2	**30**	**M**	**37/58**	**41/60**	**7/60**	**59/60**	**59/60**	**37/54**	**33/52**	**13/54**	**49/55**	**39/53**	**Sham**
			p=0.048*	**p=0.006***	**p<0.001***	**p<0.001***	**p<0.001***	**p=0.009***	**p=0.070**	**p<0.001***	**p<0.001***	**p<0.001***	
			18/28	**24/37**	**12/41**	**30/32**	**28/31**	**37/54**	**40/52**	**33/56**	**40/54**	**30/52**	**7 Hz**
			p=0.185	**p=0.099**	**p=0.012***	**p<0.001***	**p<0.001***	**p=0.009***	**p<0.001***	**p=0.229**	**p<0.001***	**p=0.332**	

			48/58	38/58	12/59	58/60	55/59	42/57	35/59	24/57	48/57	37/55	18 Hz
			p<0.001*	p=0.025*	p<0.001*	p<0.001*	p<0.001*	p<0.001*	p=0.193	p=0.289	p<0.001*	p=0.015*	
3	22	F	45/59	49/59	10/58	56/58	52/58	32/58	30/55	8/57	49/55	36/59	Sham
			p<0.001*	p<0.001*	p<0.001*	p<0.001*	p<0.001*	p=0.512	p=0.590	p<0.001*	p<0.001*	p=0.117	
			44/57	39/48	8/57	53/56	52/56	34/55	38/55	17/55	47/57	41/57	7 Hz
			p<0.001*	p<0.001*	p<0.001*	p<0.001*	p<0.001*	p=0.105	p=0.006*	p=0.006*	p<0.001*	p=0.001*	
			34/49	34/42	14/55	54/55	40/49	32/51	23/40	14/51	39/43	32/43	18 Hz
			p=0.009*	p<0.001*	p<0.001*	p<0.001*	p<0.001*	p=0.092	p=0.430	p=0.001*	p<0.001*	p=0.002*	
4	22	F	31/60	32/59	16/58	45/60	43/59	29/60	37/59	31/59	32/60	32/60	Sham
			p=0.897	p=0.603	p<0.001*	p<0.001*	p<0.001*	p=0.897	p=0.067	p=0.795	p=0.699	p=0.699	
			35/59	33/60	16/59	52/60	49/60	31/60	31/60	46/60	17/60	17/60	7 Hz
			p=0.193	p=0.519	p<0.001*	p<0.001*	p<0.001*	p=0.897	p=0.897	p<0.001*	p=0.001*	p=0.001*	
			34/59	36/60	25/60	49/58	47/59	28/60	38/60	41/59	23/60	21/60	18 Hz
			p=0.298	p=0.155*	p=0.245	p<0.001*	p<0.001*	p=0.699	p=0.052	p=0.004*	p=0.092	p=0.027*	
5	24	M	31/59	31/60	31/60	37/60	33/59	35/59	43/59	29/58	37/59	28/60	Sham
			p=0.795	p=0.897	p=0.897	p=0.092	p=0.435	p=0.193	p=0.001*	p=1.000	p=0.067	p=0.699	
			27/58	31/58	28/59	26/58	28/59	33/57	27/60	31/60	32/59	34/58	7 Hz
			p=0.694	p=0.694	p=0.795	p=0.512	p=0.795	p=0.289	p=0.519	p=0.897	p=0.603	p=0.237	
			31/60	29/56	34/58	34/58	27/53	36/58	37/56	26/58	39/57	30/56	18 Hz
			p=0.897	p=0.894	p=0.237	p=0.237	p=1.000	p=0.087	p=0.022*	p=0.512	p=0.008*	p=0.689	
6	23	F	36/60	30/55	17/56	41/60	37/57	35/58	31/58	33/57	38/58	29/57	Sham
			p=0.155	p=0.590	p=0.005*	p=0.006*	p=0.033*	p=0.148	p=0.694	p=0.289	p=0.025*	p=1.000	

			35/58	34/60	27/59	39/60	41/59	33/59	31/59	36/59	27/59	29/60	7 Hz
			p=0.148	p=0.366	p=0.603	p=0.027*	p=0.004*	p=0.559	p=0.795	p=0.117	p=0.603	p=0.897	
			31/60	39/58	26/56	46/57	42/59	38/60	37/59	27/59	30/60	34/60	18 Hz
			p=0.897	p=0.012*	p=0.689	p<0.001*	p=0.002*	p=0.052	p=0.067	p=0.603	p=1.000	p=0.366	
7	24	F	36/57	39/58	21/59	56/59	51/59	47/60	53/60	51/59	43/60	19/60	Sham
			p=0.063	p=0.012*	p=0.036*	p<0.001*	p<0.001*	p<0.001*	p<0.001*	p<0.001*	p=0.001*	p<0.001*	
			45/58	36/51	27/54	54/56	42/52	48/58	43/58	54/59	24/60	14/59	7 Hz
			p<0.001*	p=0.005*	p=1.000	p<0.001*	p<0.001*	p<0.001*	p<0.001*	p<0.001*	p=0.155	p<0.001*	
			44/59	34/58	26/59	56/60	51/60	50/59	48/59	59/60	35/60	16/59	18 Hz
			p<0.001*	p=0.237	p=0.435	p<0.001*	p<0.001*	p<0.001*	p<0.001*	p<0.001*	p=0.245	p<0.001*	
8	22	F	50/59	51/60	22/60	57/60	56/60	34/60	39/59	22/60	40/60	29/60	Sham
			p<0.001*	p<0.001*	p=0.052	p<0.001*	p<0.001*	p=0.366	p=0.018*	p=0.052	p=0.013*	p=0.897	
			37/60	36/60	23/60	44/59	41/57	38/58	43/60	25/60	55/60	41/59	7 Hz
			p=0.092	p=0.115	p=0.092	p<0.001*	p=0.001*	p=0.025*	p=0.001*	p=0.245	p<0.001*	p=0.004*	
			45/60	42/60	30/60	52/60	40/60	40/60	50/60	20/60	56/60	48/60	18 Hz
			p<0.001*	p=0.003*	p=1.000	p<0.001*	p=0.013*	p=0.013*	p<0.001*	p=0.013*	p<0.001*	p<0.001*	
9	25	F	43/60	40/59	22/60	53/60	47/60	37/60	30/59	47/59	37/59	32/59	Sham
			p<0.001*	p=0.009*	p=0.052	p<0.001*	p<0.001*	p=0.092	p=1.000	p<0.001*	p=0.067	p=0.603	
			30/59	29/59	7/60	54/58	49/60	33/60	35/60	25/60	34/60	41/60	7 Hz
			p=1.000	p=1.000	p<0.001*	p<0.001*	p<0.001*	p=0.519	p=0.245	p=0.245	p=0.366	p=0.006*	
			46/59	43/60	9/60	58/59	54/60	33/60	40/60	48/60	43/60	37/60	18 Hz
			p<0.001*	p=0.001*	p<0.001*	p<0.001*	p<0.001*	p=0.519	p=0.013*	p<0.001*	p=0.001*	p=0.092	

10	**24**	**F**	**35/60**	**33/59**	**19/60**	**37/60**	**46/60**	**31/60**	**35/59**	**17/59**	**46/60**	**41/60**	**Sham**
			p=0.245	**p=0.435**	**p=0.006***	**p=0.092**	**p<0.001***	**p=0.897**	**p=0.193**	**p=0.002***	**p<0.001***	**p=0.006***	
			38/60	**39/59**	**13/60**	**55/59**	**52/58**	**33/60**	**35/60**	**18/60**	**50/59**	**51/60**	**7 Hz**
			p=0.052	**p=0.018***	**p<0.001***	**p<0.001***	**p<0.001***	**p=0.519**	**p=0.245**	**p=0.003***	**p<0.001***	**p<0.001***	
			44/60	**39/60**	**20/60**	**45/60**	**48/59**	**38/60**	**33/60**	**26/59**	**43/59**	**38/59**	**18 Hz**
			p<0.001*	**p=0.027***	**p=0.013***	**p<0.001***	**p<0.001***	**p=0.052**	**p=0.519**	**p=0.435**	**p=0.001***	**p=0.036***	
11	**24**	**F**	**29/58**	**33/58**	**33/57**	**29/59**	**26/59**	**37/60**	**42/59**	**40/59**	**16/60**	**24/60**	**Sham**
			p=1.000	**p=0.358**	**p=0.289**	**p=1.000**	**p=0.435**	**p=0.092**	**p=0.002***	**p=0.009***	**p<0.001***	**p=0.155**	
			38/60	**37/58**	**43/57**	**28/58**	**52/58**	**32/60**	**38/60**	**53/59**	**21/60**	**24/60**	**7 Hz**
			p=0.052	**p=0.048***	**p<0.001***	**p=0.896**	**p<0.001***	**p=0.699**	**p=0.052**	**p<0.001***	**p=0.027***	**p=0.155**	
			26/59	**33/59**	**31/58**	**30/59**	**33/59**	**27/56**	**30/58**	**34/60**	**24/56**	**27/58**	**18 Hz**
			p=0.435	**p=0.435**	**p=0.694**	**p=1.000**	**p=0.435**	**p=0.894**	**p=0.896**	**p=0.366**	**p=0.350**	**p=0.694**	
12	**23**	**M**	**43/58**	**36/54**	**44/54**	**41/57**	**25/57**	**30/58**	**40/59**	**49/60**	**20/59**	**19/57**	**Sham**
			p<0.001*	**p=0.020***	**p<0.001***	**p=0.001***	**p=0.427**	**p=0.896**	**p=0.009***	**p<0.001***	**p=0.018***	**p=0.016***	
			40/59	**42/60**	**51/60**	**31/60**	**19/58**	**33/60**	**45/59**	**53/59**	**13/59**	**11/60**	**7 Hz**
			p=0.009*	**p=0.003***	**p<0.001***	**p=0.897**	**p=0.012***	**p=0.519**	**p<0.001***	**p<0.001***	**p<0.001***	**p<0.001***	
			39/59	**47/58**	**52/58**	**23/59**	**15/60**	**42/60**	**47/60**	**9/60**	**54/59**	**11/60**	**18 Hz**
			p=0.018*	**p<0.001***	**p<0.001***	**p=0.117**	**p<0.001***	**p=0.003***	**p<0.001***	**p<0.001***	**p<0.001***	**p<0.001***	
13	**22**	**F**	**51/60**	**50/60**	**0/60**	**59/59**	**60/60**	**28/60**	**33/60**	**5/60**	**58/59**	**54/60**	**Sham**
			p<0.001*	**p<0.001***	**p<0.001***	**p=0.001***	**p=0.427**	**p=0.699**	**p=0.519**	**p<0.001***	**p<0.001***	**p<0.001***	
			39/60	**42/60**	**4/60**	**59/59**	**57/60**	**33/59**	**35/60**	**11/59**	**50/60**	**48/60**	**7 Hz**
			p=0.027*	**p=0.003***	**p<0.001***	**p<0.001***	**p<0.001***	**p=0.435**	**p=0.245**	**p<0.001***	**p<0.001***	**p<0.001***	

			47/59	52/59	1/60	59/60	58/59	36/58	32/59	3/59	57/60	51/59	18 Hz
			p<0.001*	p<0.001*	p<0.001*	p<0.001*	p<0.001*	p=0.087	p=0.603	p<0.001*	p<0.001*	p<0.001*	
14	23	F	50/60	44/59	10/60	60/60	56/60	31/60	28/59	5/60	57/60	47/60	Sham
			p<0.001*	p<0.001*	p<0.001*	p<0.001*	p<0.001*	p=0.897	p=0.795	p<0.001*	p<0.001*	p<0.001*	
			44/60	42/58	12/60	53/60	55/59	35/57	34/55	22/58	44/58	39/55	7 Hz
			p<0.001*	p=0.001*	p<0.001*	p<0.001*	p<0.001*	p=0.111	p=0.105	p=0.087	p<0.001*	p=0.003*	
			40/60	48/60	6/59	60/60	56/60	27/60	34/59	8/60	56/60	51/60	18 Hz
			p=0.013*	p<0.001*	p<0.001*	p<0.001*	p<0.001*	p=0.519	p=0.298	p<0.001*	p<0.001*	p<0.001*	
15	23	F	40/59	32/59	5/59	58/60	60/60	47/60	48/58	57/58	17/59	13/60	Sham
			p=0.009*	p=0.603	p<0.001*	p<0.001*	p<0.001*	p<0.001*	p<0.001*	p<0.001*	p=0.002*	p<0.001*	
			43/59	35/57	4/59	59/60	57/59	45/59	49/57	54/59	34/59	12/60	7 Hz
			p=0.001*	p=0.111	p<0.001*	p<0.001*	p<0.001*	p<0.001*	p<0.001*	p<0.001*	p<0.001*	p<0.001*	
			44/58	48/60	6/56	56/59	57/60	38/55	36/56	47/57	25/56	21/55	18 Hz
			p<0.001*	p<0.001*	p<0.001*	p<0.001*	p<0.001*	p=0.006*	p=0.044*	p<0.001*	p=0.504	p=0.105	
16	25	F	44/58	38/49	14/59	59/59	56/60	41/57	47/59	51/60	35/58	22/60	Sham
			p<0.001*	p<0.001*	p<0.001*	p<0.001*	p<0.001*	p=0.001*	p<0.001*	p<0.001*	p=0.148	p=0.052	
			44/58	44/58	9/60	60/60	56/60	39/58	39/60	36/58	45/59	30/58	7 Hz
			p<0.001*	p<0.001*	p<0.001*	p<0.001*	p<0.001*	p=0.012*	p=0.027*	p=0.087	p<0.001*	p=0.896	
			44/60	46/58	5/59	60/60	56/60	48/60	45/57	43/59	39/57	28/59	18 Hz
			p<0.001*	p<0.001*	p<0.001*	p<0.001*	p<0.001*	p<0.001*	p<0.001*	p=0.001*	p=0.008*	p=0.795	
17	24	M	52/56	49/54	22/58	56/59	51/58	28/45	34/40	37/46	24/41	15/37	Sham
			p<0.001*	p<0.001*	p=0.087	p<0.001*	p<0.001*	p=0.135	p<0.001*	p<0.001*	p=0.349	p=0.324	

			53/60	56/59	16/59	60/60	56/60	37/60	49/60	49/60	30/60	31/59	7 Hz
			p<0.001*	p<0.001*	p=0.001*	p<0.001*	p<0.001*	p=0.092	p<0.001*	p<0.001*	p=1.000	p=0.795	
			48/60	48/59	22/59	59/59	58/59	35/59	38/60	45/60	24/60	22/60	18 Hz
			p<0.001*	p<0.001*	p=0.067	p<0.001*	p<0.001*	p=0.193	p=0.052	p<0.001*	p=0.155	p=0.052	
18	35	F	43/60	44/60	28/59	50/60	35/60	31/60	33/60	27/60	45/60	36/59	Sham
			p=0.001*	p<0.001*	p=0.795	p<0.001*	p=0.245	p=0.897	p=0.519	p=0.519	p<0.001*	p=0.117	
			35/60	35/60	2/60	59/60	57/60	31/60	35/60	15/60	49/60	52/60	7 Hz
			p=0.245	p=0.245	p<0.001*	p<0.001*	p<0.001*	p=0.897	p=0.245	p<0.001*	p<0.001*	p<0.001*	
			41/60	34/58	11/60	49/59	51/59	38/59	31/60	12/59	51/60	43/60	18 Hz
			p=0.006*	p=0.237	p<0.001*	p<0.001*	p<0.001*	p=0.036	p=0.897	p<0.001*	p<0.001*	p=0.001*	
19	22	F	32/60	33/60	20/59	42/57	39/58	32/60	33/60	28/59	42/60	24/59	Sham
			p=0.699	p=0.519	p=0.018*	p<0.001*	p=0.012*	p=0.699	p=0.519	p=0.795	p=0.003*	p=0.193	
			32/57	19/57	16/59	49/58	41/58	33/59	31/59	25/58	31/59	26/58	7 Hz
			p=0.427	p=0.016*	p=0.001*	p<0.001*	p=0.002*	p=0.435	p=0.795	p=0.358	p=0.795	p=0.512	
			30/58	33/60	11/60	44/60	48/60	29/58	28/60	16/60	41/58	35/59	18 Hz
			p=0.896	p=0.519	p<0.001*	p<0.001*	p<0.001*	p=1.000	p=0.699	p<0.001*	p=0.002*	p=0.193	
20	24	F	39/60	35/59	19/60	53/59	50/60	34/60	35/60	31/58	44/60	31/59	Sham
			p=0.018*	p=0.193	p=0.006*	p<0.001*	p<0.001*	p=0.366	p=0.245	p=0.694	p<0.001*	p=0.897	
			41/60	48/60	19/59	55/59	50/59	33/60	36/59	31/59	36/60	27/57	7 Hz
			p=0.006*	p<0.001*	p=0.009*	p<0.001*	p<0.001*	p=0.519	p=0.117	p=0.795	p=0.155	p=0.791	
			35/60	33/59	14/60	54/60	54/60	31/59	39/60	37/60	32/58	26/60	18 Hz
			p=0.245	p=0.435	p<0.001*	p<0.001*	p<0.001*	p=0.795	p=0.027*	p=0.092	p=0.512	p=0.366	

21	**23**	**F**	**29/60**	**38/60**	**19/60**	**40/59**	**43/58**	**32/59**	**35/58**	**31/59**	**35/60**	**38/60**	**Sham**
			p=0.897	**p=0.052**	**p=0.006***	**p=0.009***	**p<0.001***	**p=0.603**	**p=0.148**	**p=0.795**	**p=0.245**	**p=0.052**	
			29/59	**38/60**	**21/60**	**47/60**	**40/59**	**29/60**	**31/60**	**22/59**	**48/57**	**37/60**	**7 Hz**
			p=1.000	**p=0.052**	**p=0.027***	**p<0.001***	**p=0.009***	**p=0.897**	**p=0.897**	**p=0.067**	**p<0.001***	**p=0.092**	
			38/60	**38/59**	**20/58**	**54/60**	**48/60**	**27/58**	**34/59**	**31/59**	**34/59**	**34/60**	**18 Hz**
			p=0.052	**p=0.036***	**p=0.025***	**p<0.001***	**p<0.001***	**p=0.694**	**p=0.298**	**p=0.795**	**p=0.298**	**p=0.366**	
22	**24**	**F**	**30/58**	**29/59**	**26/59**	**33/58**	**30/58**	**29/59**	**28/59**	**34/60**	**29/56**	**27/58**	**Sham**
			p=0.896	**p=1.000**	**p=0.435**	**p=0.358**	**p=0.896**	**p=1.000**	**p=0.795**	**p=0.366**	**p=0.894**	**p=0.694**	
			29/59	**33/60**	**35/58**	**29/58**	**27/60**	**30/58**	**25/59**	**31/57**	**32/58**	**34/59**	**7 Hz**
			p=1.000	**p=0.519**	**p=0.148**	**p=1.000**	**p=0.519**	**p=0.896**	**p=0.298**	**p=0.597**	**p=0.512**	**p=0.298**	
			35/60	**30/60**	**26/60**	**40/59**	**34/59**	**32/60**	**36/60**	**32/59**	**32/60**	**26/60**	**18 Hz**
			p=0.245	**p=1.000**	**p=0.366**	**p=0.009***	**p=0.298**	**p=0.699**	**p=0.155**	**p=0.603**	**p=0.699**	**p=0.366**	
23	**24**	**F**	**44/60**	**44/59**	**9/60**	**59/60**	**53/60**	**33/60**	**30/56**	**25/60**	**47/58**	**34/59**	**Sham**
			p<0.001*	**p<0.001***	**p<0.001***	**p<0.001***	**p<0.001***	**p=0.519**	**p=0.689**	**p=0.245**	**p=0.048***	**p=0.298**	
			43/57	**39/57**	**18/60**	**54/60**	**51/59**	**28/58**	**29/60**	**25/58**	**36/60**	**31/58**	**7 Hz**
			p<0.001*	**p=0.008***	**p=0.003***	**p<0.001***	**p<0.001***	**p=0.896**	**p=0.897**	**p=0.358**	**p=0.155**	**p=0.694**	
			40/58	**48/58**	**7/58**	**49/58**	**52/58**	**32/59**	**28/58**	**25/59**	**35/60**	**36/58**	**18 Hz**
			p=0.005*	**p<0.001***	**p<0.001***	**p<0.001***	**p<0.001***	**p=0.603**	**p=0.896**	**p=0.298**	**p=0.245**	**p=0.087**	
24	**22**	**F**	**33/60**	**36/59**	**7/60**	**54/59**	**52/59**	**29/60**	**28/60**	**26/60**	**39/59**	**39/58**	**Sham**
			p=0.519	**p=0.117**	**p<0.001***	**p<0.001***	**p<0.001***	**p=0.897**	**p=0.699**	**p=0.366**	**p=0.018***	**p=0.012***	
			34/57	**41/56**	**7/60**	**58/60**	**50/60**	**28/60**	**25/59**	**27/59**	**35/59**	**32/58**	**7 Hz**
			p=0.185	**p=0.001***	**p<0.001***	**p<0.001***	**p<0.001***	**p=0.699**	**p=0.298**	**p=0.603**	**p=0.193**	**p=0.512**	

			32/60	24/55	32/57	33/58	26/56	29/59	33/58	40/60	18/56	22/60	18 Hz
			p=0.699	p=0.419	p=0.427	p=0.358	p=0.689	p=1.000	p=0.358	p=0.013*	p=0.010*	p=0.087	
25	22	F	26/59	28/60	24/60	34/60	34/60	30/60	22/59	29/59	29/59	33/59	Sham
			p=0.435	p=0.699	p=0.155	p=0.366	p=0.366	p=1.000	p=0.067	p=1.000	p=1.000	p=0.435	
			37/60	22/59	29/60	39/59	35/59	29/60	25/60	28/59	32/60	31/60	7 Hz
			p=0.092	p=0.067	p=0.897	p=0.018*	p=0.193	p=0.897	p=0.245	p=0.795	p=0.699	p=0.897	
			27/60	26/59	18/60	35/60	36/59	30/60	28/60	31/59	30/60	30/60	18 Hz
			p=0.519	p=0.435	p=0.003*	p=0.245	p=0.117	p=1.000	p=0.699	p=0.795	p=1.000	p=1.000	
26	21	M	41/56	51/60	11/59	59/60	58/59	34/59	47/59	50/57	37/60	21/59	Sham
			p=0.001*	p<0.001*	p<0.001*	p<0.001*	p<0.001*	p=0.298	p<0.001*	p<0.001*	p=0.092	p=0.036*	
			40/49	48/56	11/56	54/54	52/54	35/59	51/59	42/59	34/60	28/59	7 Hz
			p<0.001*	p<0.001*	p<0.001*	p<0.001*	p<0.001*	p=0.193	p<0.001*	p=0.002*	p=0.366	p=0.795	
			38/53	49/57	11/52	56/57	57/59	37/56	39/55	33/54	31/52	26/50	18 Hz
			p=0.002*	p<0.001*	p<0.001*	p<0.001*	p<0.001*	p=0.022*	p=0.003*	p=0.134	p=0.212	p=0.888	
27	29	F	32/60	32/58	25/60	29/60	28/60	34/59	36/60	33/60	34/60	31/59	Sham
			p=0.699	p=0.512	p=0.245	p=0.897	p=0.699	p=0.298	p=0.155	p=0.519	p=0.366	p=0.795	
			39/59	37/57	12/57	49/60	39/60	35/60	36/60	19/59	39/60	36/60	7 Hz
			p=0.018*	p=0.033*	p<0.001*	p<0.001*	p=0.027*	p=0.245	p=0.155	p=0.009*	p=0.027*	p=0.155	
			46/59	34/59	8/60	57/60	54/57	42/59	40/60	22/59	46/59	36/59	18 Hz
			p<0.001*	p=0.298	p<0.001*	p<0.001*	p<0.001*	p=0.002*	p=0.013*	p=0.067	p<0.001*	p=0.117	
28	22	F	42/58	41/58	14/58	53/57	55/59	31/58	40/58	41/57	28/59	26/57	Sham
			p=0.001*	p=0.002*	p<0.001*	p<0.001*	p<0.001*	p=0.694	p=0.005*	p=0.001*	p=0.795	p=0.597	

			25/60	32/58	26/59	29/60	24/60	21/59	28/59	28/60	39/59	32/59	7 Hz
			p=0.245	p=0.512	p=0.435	p=0.897	p=0.155	p=0.036*	p=0.795	p=0.699	p=0.018*	p=0.603	
			43/60	45/60	10/60	58/60	57/60	29/60	30/60	34/60	36/59	36/60	18 Hz
			p=0.001*	p<0.001*	p<0.001*	p<0.001*	p<0.001*	p=0.897	p=1.000	p=0.366	p=0.117	p=0.155	
29	24	F	40/60	40/60	28/60	49/60	51/60	35/59	47/60	32/60	43/60	37/60	Sham
			p=0.013*	p=0.013*	p=0.699	p<0.001*	p<0.001*	p=0.193	p<0.001*	p=0.699	p=0.001*	p=0.092	
			50/60	46/60	11/60	58/60	58/60	33/59	34/57	18/57	42/59	32/59	7 Hz
			p<0.001*	p<0.001*	p<0.001*	p<0.001*	p<0.001*	p=0.435	p=0.185	p=0.008*	p=0.002*	p=0.603	
			48/60	43/60	24/60	54/60	49/60	27/59	30/58	27/58	38/58	32/59	18 Hz
			p<0.001*	p=0.001*	p=0.155	p<0.001*	p<0.001*	p=0.603	p=0.896	p=0.694	p=0.358	p=0.603	
30	24	F	53/60	46/60	16/60	54/58	57/60	39/60	38/60	43/59	29/60	19/60	Sham
			p<0.001*	p<0.001*	p<0.001*	p<0.001*	p<0.001*	p=0.027*	p=0.052	p=0.001*	p=0.897	p=0.006*	
			49/60	42/60	10/60	59/60	56/60	33/59	40/59	40/58	22/59	27/57	7 Hz
			p<0.001*	p=0.003*	p<0.001*	p<0.001*	p<0.001*	p=0.435	p=0.009*	p=0.005*	p=0.067	p=0.791	
			45/60	43/60	8/60	59/60	60/60	30/60	24/60	14/60	47/60	40/60	18 Hz
			p<0.001*	p=0.001*	p<0.001*	p<0.001*	p<0.001*	p=1.000	p=0.155	p<0.001*	p<0.001*	p=0.013*	
31	23	F	40/60	47/59	9/60	56/60	55/60	42/60	38/59	16/60	56/60	45/58	Sham
			p=0.013*	p<0.001*	p<0.001*	p<0.001*	p<0.001*	p=0.003*	p=0.036*	p<0.001*	p<0.001*	p<0.001*	
			27/54	45/59	24/56	40/57	48/59	35/57	33/50	11/58	53/56	42/54	7 Hz
			p=1.000	p<0.001*	p=0.350	p=0.003*	p<0.001*	p=0.111	p=0.033*	p<0.001*	p<0.001*	p<0.001*	
			41/60	48/60	9/60	59/60	57/60	38/60	43/60	14/59	52/60	43/60	18 Hz
			p=0.006*	p<0.001*	p<0.001*	p<0.001*	p<0.001*	p=0.052	p=0.001*	p<0.001*	p<0.001*	p=0.001*	

32	**22**	**F**	**38/59**	**41/59**	**15/59**	**51/57**	**51/58**	**34/60**	**42/60**	**36/57**	**31/59**	**26/60**	**Sham**
			p=0.036*	**p=0.004***	**p<0.001***	**p<0.001***	**p<0.001***	**p=0.366**	**p=0.003***	**p=0.063**	**p=0.795**	**p=0.366**	
			37/60	**41/60**	**12/59**	**57/60**	**48/60**	**33/59**	**31/60**	**37/60**	**30/60**	**29/30**	**7 Hz**
			p=0.092	**p=0.006***	**p<0.001***	**p<0.001***	**p<0.001***	**p=0.435**	**p=0.897**	**p=0.092**	**p=1.000**	**p<0.001***	
			43/60	**45/59**	**9/58**	**57/60**	**58/60**	**37/60**	**38/58**	**50/59**	**23/57**	**18/58**	**18 Hz**
			p=0.001*	**p<0.001***	**p<0.001***	**p<0.001***	**p<0.001***	**p=0.092**	**p=0.025***	**p<0.001***	**p=0.185**	**p=0.005***	
33	**25**	**F**	**47/60**	**51/60**	**11/59**	**59/60**	**57/60**	**35/60**	**43/60**	**24/60**	**44/60**	**45/58**	**Sham**
			p<0.001*	**p<0.001***	**p<0.001***	**p<0.001***	**p<0.001***	**p=0.245**	**p=0.001***	**p=0.155**	**p<0.001***	**p<0.001***	
			42/60	**54/59**	**12/60**	**60/60**	**56/60**	**29/60**	**36/60**	**25/60**	**48/60**	**42/60**	**7 Hz**
			p=0.003*	**p<0.001***	**p<0.001***	**p<0.001***	**p<0.001***	**p=0.897**	**p=0.155**	**p=0.245**	**p<0.001***	**p=0.003***	
			43/58	**48/58**	**23/58**	**55/59**	**56/59**	**33/59**	**33/59**	**22/59**	**45/60**	**36/59**	**18 Hz**
			p<0.001*	**p<0.001***	**p=0.148**	**p<0.001***	**p<0.001***	**p=0.435**	**p=0.435**	**p=0.067**	**p<0.001***	**p=0.117**	
34	**26**	**F**	**45/59**	**40/59**	**12/59**	**56/59**	**56/59**	**48/60**	**46/60**	**17/59**	**56/59**	**53/60**	**Sham**
			p<0.001*	**p=0.009***	**p<0.001***	**p<0.001***	**p<0.001***	**p<0.001***	**p<0.001***	**p=0.002***	**p<0.001***	**p<0.001***	
			41/59	**41/58**	**13/56**	**51/57**	**47/56**	**41/60**	**35/60**	**18/60**	**47/60**	**51/60**	**7 Hz**
			p=0.004*	**p=0.003***	**p<0.001***	**p<0.001***	**p<0.001***	**p=0.006***	**p=0.245**	**p=0.003***	**p<0.001***	**p<0.001***	
			47/60	**45/60**	**15/60**	**56/60**	**51/60**	**43/60**	**43/60**	**25/60**	**58/60**	**47/60**	**18 Hz**
			p<0.001*	**p<0.001***	**p<0.001***	**p<0.001***	**p<0.001***	**p=0.001***	**p=0.001***	**p=0.245**	**p<0.001***	**p<0.001***	

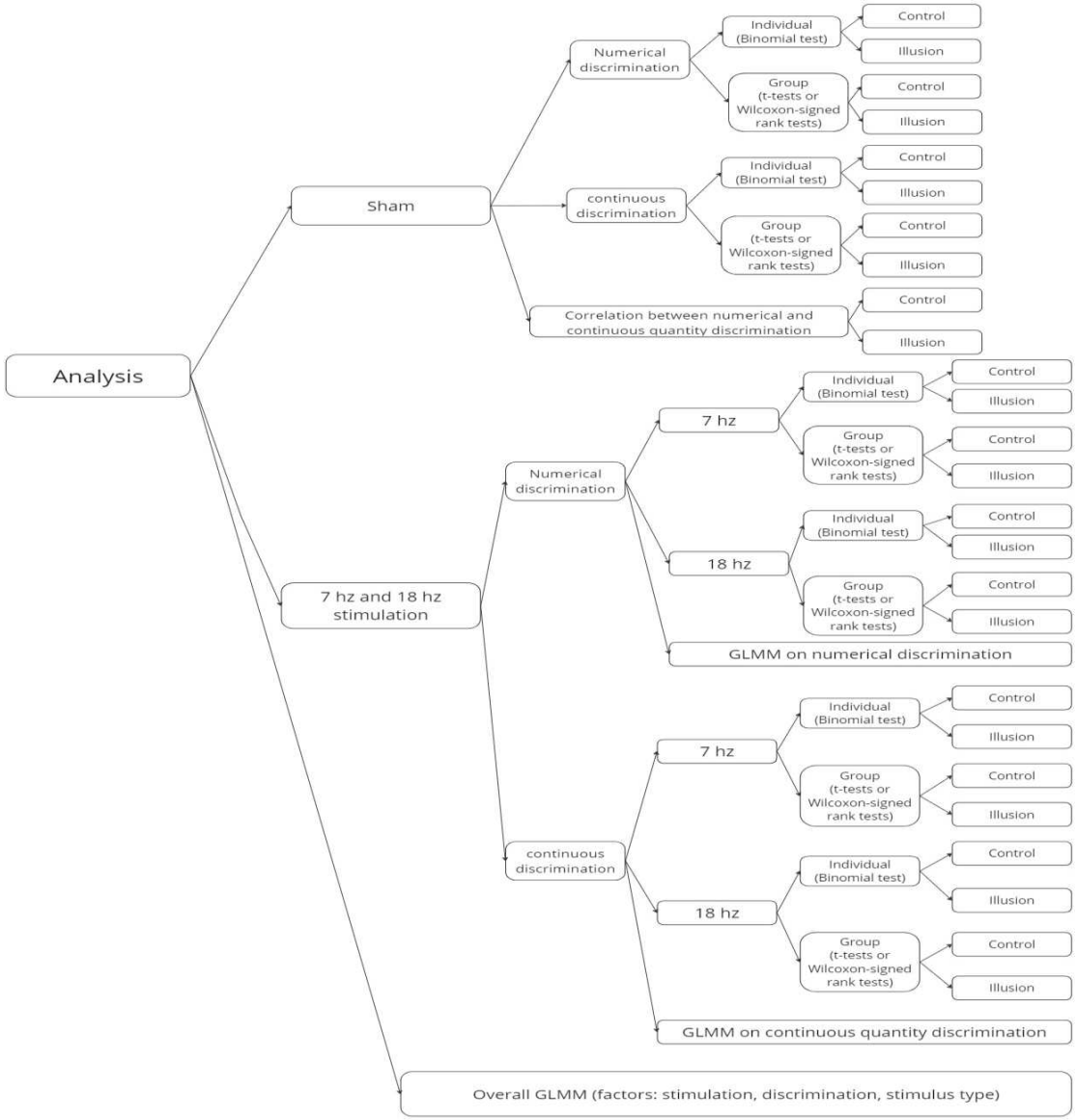

Figure S1. This figure represents a schematization of the analyses that have been conducted.

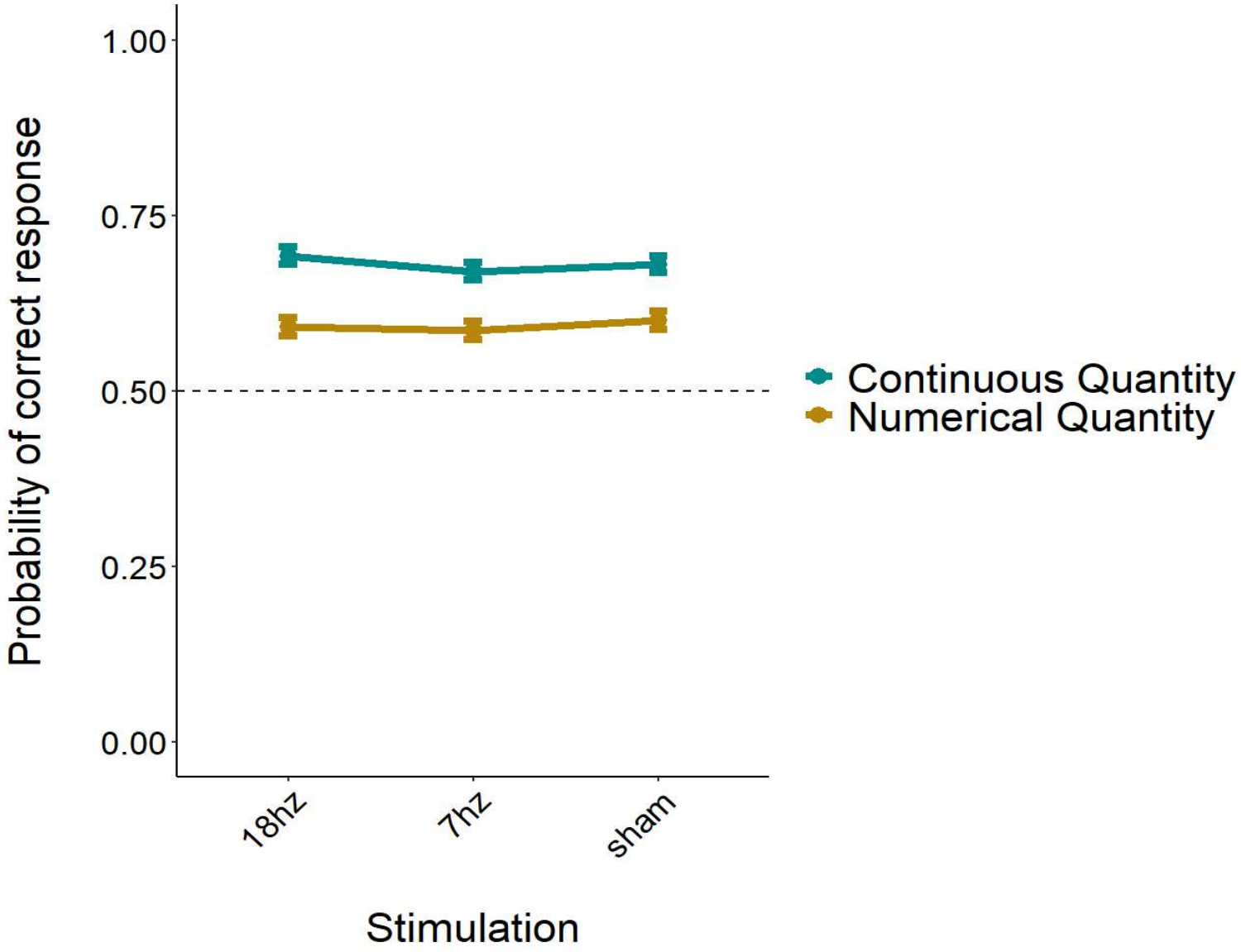

Figure S2. Comparison of the performances (mean ± SE) with the three stimulation frequencies for both type of discrimination tasks.